energies

MDPI

Article

Influence of Blending Model *n*-Butanol Alcoholysis Derived Advanced Biofuel Blends with Diesel on the Regulated Emissions from a Diesel Hybrid Vehicle †

Scott Wiseman [1], Karl Ropkins [2], Hu Li [1] and Alison S. Tomlin [1,*]

[1] School of Chemical and Process Engineering, University of Leeds, Woodhouse Lane, Leeds LS2 9JT, UK; s.wiseman@leeds.ac.uk (S.W.); h.li3@leeds.ac.uk (H.L.)
[2] Institute for Transport Studies, University of Leeds, Woodhouse Lane, Leeds LS2 9JT, UK; k.ropkins@leeds.ac.uk
* Correspondence: a.s.tomlin@leeds.ac.uk
† This paper is an extended version of our paper 'Influence of Blending n-Butanol Alcoholysis Derived Advanced Biofuels with Diesel on the Regulated Emissions from a Diesel Hybrid Vehicle' presented at the 23rd European Combustion Meeting, Edinburgh, Scotland, UK, 7–10 April 2025.

Abstract

Decarbonisation of the transport sector, whilst reducing pollutant emissions, will likely involve the utilisation of multiple strategies, including hybridisation and the use of alternative fuels such as advanced biofuels as mandated by the EU. Alcoholysis of lignocellulosic feedstocks, using *n*-butanol as the solvent, can produce such potential advanced biofuel blends. Butyl blends, consisting of *n*-butyl levulinate (*n*BL), di-*n*-butyl ether, and *n*-butanol, were selected for this study. Three butyl blends with diesel, two at 10 vol% biofuel and one at 25 vol% biofuel, were tested in a Euro 6b-compliant diesel hybrid vehicle to determine the influence of the blends on regulated emissions and fuel economy. Real Driving Emissions (RDE) were measured for three cold start tests with each fuel using a Portable Emissions Measurement System (PEMS) for carbon monoxide (CO), particle number (PN), and nitrogen oxides (NO_X = NO + NO_2). When using the butyl blends, there was no noticeable change in vehicle drivability and only a small fuel economy penalty of up to 5% with the biofuel blends relative to diesel. CO, NO_X, and PN emissions were below or within one standard deviation of the Euro 6 not-to-exceed limits for all fuels tested. The CO and PN emissions reduced relative to diesel by up to 72% and 57%, respectively. NO_X emissions increased relative to diesel by up to 25% and increased with both biofuel fraction and the amount of *n*BL in that fraction. The CO emitted during the cold start period was reduced by up to 52% for the 10 vol% blends but increased by 25% when using the 25 vol% blend. NO_X and PN cold start emissions reduced relative to diesel for all three biofuel blends by up to 29% and 88%, respectively. It is envisaged that the butyl blends could reduce net carbon emissions without compromising or even improving air pollutant emissions, although optimisation of the after-treatment systems may be necessary to ensure emissions limits are met.

Keywords: advanced biofuels; real driving emissions; diesel; hybrid vehicle; gaseous emissions; portable emissions measurement system; Euro 6; *n*-butyl levulinate

Academic Editors: Paweł Droździel, Karol F. Abramek and Tomasz Osipowicz

Received: 29 October 2025
Revised: 19 December 2025
Accepted: 22 December 2025
Published: 7 January 2026

1. Introduction

Diesel vehicles have been used for decades in many applications in the transport, agriculture, construction, and heavy machinery sectors. Globally, the number of diesel

vehicles has fallen in the light-duty and passenger car market, but in the heavy-duty vehicle sector the numbers have increased [1]. This increase is primarily due to an increase in demand for haulage and goods transportation. Whilst fuel efficiency and pollutant emissions have improved with each generation of vehicles due to tightening legislation, the increased number of vehicles counteracts this, maintaining high GHG emissions from the transport sector [2].

Powertrain hybridisation is one technology used to improve fuel efficiency, thus potentially lowering the CO_2 emissions of vehicles by incorporating both internal combustion engines (ICE) and electric motors to power the vehicle [3–6]. Parallel hybrid vehicles are the most common, where the ICE and electric motor power the wheels and the batteries are charged by the engine and regenerative braking. There are two common light-duty parallel hybrid vehicle types: off vehicle charging (OVC), termed plug-in hybrids, and not off vehicle charging (NOVC). The number of diesel hybrid vehicles on the roads is small, with only 0.75% of all vehicles in the United Kingdom (UK) being diesel hybrid including plug-in diesel hybrids. However, hybridisation is one avenue continually being explored for heavy-duty vehicles. There is a scarcity of studies investigating the Real Driving Emissions (RDE) from diesel hybrid vehicles even though they have been available since 2012 [7]. If hybrid powertrains are going to become more common, further investigations into their RDE are required, especially when coupled with the utilisation of potential new fuels. The use of advanced biofuels in the transport sector is mandated in the European Union (EU) Renewable Energy Directive (RED III) [8]. Displacing fossil fuels with advanced biofuels could contribute towards reducing the carbon intensity of the fuels. In addition, they could also potentially improve tailpipe emissions of relevance to air quality via improved combustion coupled with the use of appropriate after-treatment systems.

Although subject to some push-back and renegotiation, both the UK and EU are proposing bans on the sale of new diesel ICE light-duty vehicles in 2030 and 2035, respectively. In the EU, the proposed ban includes hybrid vehicles that use gasoline and diesel which aligns with the UK's proposed ban on the sale of new gasoline and diesel hybrids from 2035 [6,9]. The proposed target date for zero-emission heavy-duty vehicles is 2040. However, ICEs using alternative fuels could be one possible technological route, as their use is under review [10]. In addition, there will still be a used vehicle market for ICE vehicles, as well as countries where there are no such proposed bans and other sectors requiring the use of liquid fuels. These liquid fuels need to have low lifecycle carbon emissions to meet decarbonisation targets. Keeping a diverse powertrain and fuel portfolio should enable easier decarbonisation of the transport sector.

In addition to the need to reduce GHGs from alternative fuel strategies, it is essential to continue to control air pollutant emissions. Tailpipe emissions are controlled via limits imposed from standards such as Euro 6, China 6, and Tier III US Emissions Standards, as well as through a range of regulatory and traffic management actions, including low emissions, ultra-low emissions, zero emissions, and clean air zones (LEZs, ULEZs and CAZs). Although the exact strategies vary, many of the zonal activities limit or disincentivise access to an area by what are assumed, on the basis of size, technology, and/or fuel types, to be the most polluting vehicles. Many studies have shown that these controlled zones can have a significant impact on reducing the local nitrogen oxides (NO_X = NO + NO_2) and NO_2 concentrations, with reductions of up to 20% observed in London with the introduction of the ULEZ [11–15]. In some countries, in certain zones, vehicles that are retrofitted with exhaust after-treatment systems can be granted permission to enter the zones. However, these zones are reliant on the in-use conformity of the vehicles entering them. Therefore, it is imperative that any new fuel that is used as a drop-in fuel, maintains, or ideally improves, vehicle emission levels in order to maintain their ability to enter the controlled zones.

The EU Renewable Energy Directive mandates the use of advanced biofuels produced from lignocellulosic materials and non-food materials as listed in Annex 9, where the net lifecycle carbon dioxide (CO_2) should be 50% or less of the fossil fuel they are displacing [8]. One potential process that uses Annex 9 materials and produces a potential advanced biofuel blend is acid-catalysed alcoholysis. The alcohol used in the alcoholysis dictates the products formed. *n*-butanol-based alcoholysis products, *n*-butyl levulinate (*n*BL), *n*-butanol (*n*BuOH), and di-*n*-butyl ether (DNBE) (referred to here as butyl blends) have been shown to be capable of forming blends with diesel that remain compliant with fuel standards [16]. *n*-Butyl levulinate has been targeted as a biofuel candidate for diesel due to its physical properties that meet the requirements set in diesel standards, such as kinematic viscosity, boiling point, and flash point.

The alcoholysis process can be tailored to produce different yields of the three biofuel components of interest (*n*BL, DNBE, *n*BuOH) using different reaction conditions and different catalysts. The use of the alcoholysis product blend as a diesel blend stock may be preferential, as less separation would be needed, thus improving the sustainability of alcoholysis. Sulphuric acid catalysed alcoholysis can produce high yields of *n*BL from a range of different feedstocks but has the drawback of being a homogeneous catalyst that requires neutralisation and removal from the product mixture. Higher yields of *n*BL are typically obtained at higher reaction temperatures (around 190 °C using traditional heating methods) with sulphuric acid as the catalyst [17–20]. The use of microwave heating has been explored, which shortens reaction times whilst achieving similar *n*BL yields. Using different heating techniques may improve the overall sustainability of the process due to their different energy demands, thus reducing lifecycle GHG emissions. The use of heterogeneous catalysts could further improve the sustainability of the process as they could be separated and recycled more readily than a homogenous catalyst such as sulphuric acid. The yield of alkyl levulinate from alcoholysis of lignocellulosic biomass is dependent on the biomass feedstock used [17–20]. Yields of *n*BL are typically higher from pure monosaccharides compared to cellulose and lignocellulosic biomass. Therefore, there may be a desire to extract the monosaccharides from the biomass to increase the levulinate yield. Each feedstock would have an optimum operating condition for a given catalyst, and this would need to be determined for a range of feedstocks to ensure the overall sustainability of *n*BL production for different locations with potential differences in feedstock availability [17–20].

Different compositions of potential butyl blends from alcoholysis have been used in several small engine studies with differing results, showing both increases and reductions in legislated emissions. For example, Antonetti et al. [21] studied the utilisation of a butyl-based blend consisting of 70 wt% *n*BuOH, 20 wt% DNBE, and 10 wt% *n*BL, blended with an EN 590 diesel at 10 to 30 vol%. When these blends were tested in a two-cylinder engine at engine speeds between 1500 and 2500 rpm, the fuel smoke number and carbon monoxide (CO) emissions reduced relative to diesel as the biofuel fraction increased. NO_X and hydrocarbon (HC) emissions remained similar to those of diesel. However, a blend with this high fraction of *n*BuOH is unlikely to meet the flash point limit of EN 590 [16,22]. In contrast, Wiseman et al. [23] tested a range of butyl blends with diesel at 10 and 25 vol% biofuel which met the flash point, density, and viscosity limits of BS 2869 and EN 590. When the butyl blends with diesel were tested in a single-cylinder generator set (genset) engine at 3000 rpm, the CO and total hydrocarbon emissions increased with increasing *n*BL and biofuel fraction, whereas the particle number (PN) and $PM_{2.5}$ mass emissions reduced, with NO_X emissions remaining similar to those of diesel. Therefore, the use of high *n*BL fractions would require more effective emissions control of CO and HC emissions, which would be expected from a Euro 6 vehicle which has appropriate exhaust after-treatment

systems. Additionally, the injection pressure in a vehicle will be approximately 10 times that used in the genset tested. This should improve fuel atomisation, favouring more complete combustion and thus potentially reducing or even preventing increases in engine-out CO and hydrocarbon emissions that were observed from the genset testing relative to diesel [24].

With emissions limits becoming more stringent with each generation of the standards, the after-treatment systems in diesel vehicles have become increasingly more complex and sophisticated. The light-duty vehicle emissions standard Euro 6 sets strict limits on nitrogen oxides (NO_X = NO + NO_2), particle number (PN), and CO emissions. The NO_X emissions limit for light-duty vehicles reduced from 0.18 g/km in Euro 5 to 0.08 g/km in Euro 6 [25–27]. Attainment of emissions standards typically requires the use of multiple emissions control systems including selective catalytic reduction (SCR), exhaust gas recirculation (EGR), diesel particulate filters (DPFs), and diesel oxidation catalysts (DOCs) [13,28]. The compatibility of existing after-treatment systems with novel advanced biofuel candidates needs to be established if any biofuel blends are to be used as drop-in low-carbon alternatives to diesel. A new fuel could change the engine-out exhaust composition, which may produce compounds that deactivate or poison existing catalysts, resulting in higher tailpipe emissions than when running with standard diesel. Therefore, ensuring tailpipe emissions remain compliant with the Euro 6 limits when running with the butyl blends will give an indication of their compatibility with existing after-treatment systems.

Whilst there have been few studies of real-world driving emissions for diesel hybrids, Franco et al. [29] conducted real-world testing for three diesel hybrid vehicles, two Euro 5 vehicles and one Euro 6 vehicle, equipped with a gas Portable Emissions Measurement System (PEMS). All three vehicles were equipped with a DOC, a DPF, and EGR. The Euro 6 vehicle also had an SCR system. The vehicles used were type approved before the implementation of the RDE test protocol. Franco et al. [29] conducted both New European Drive Cycle (NEDC) and Worldwide Harmonised Light Vehicle Test Procedure (WLTP) laboratory testing and found that the on-road NO_X emissions factors were higher than the emissions limits for the applicable standard for all three vehicles when running with diesel. The high NO_X emissions indicate that the SCR system was not operating effectively to reduce tailpipe NO_X emissions on the road. With many vehicles globally in use being pre-RDE but Euro 6-compliant, there is a high possibility that many of these vehicles have real-world emissions that are much higher than the emissions limits. It is likely that these vehicles will remain in use for many years, therefore reducing emissions through other means such as alternative fuels should be targeted.

The addition of *n*-butanol to diesel has been tested in several Real Driving Emissions (RDE) studies. Tipanluisa et al. [30] tested a 10% *n*BuOH and diesel blend in a Euro 5b light-duty diesel van. The exhaust after-treatment system included a DOC and a DPF, and the vehicle was also equipped with EGR. Following RDE tests, the CO emissions in all three RDE phases increased when adding 10% *n*BuOH to diesel, with a 45% increase in the urban phase relative to the diesel baseline emissions. Given the presence of the DOC, these high emissions indicate that the after-treatment device could not cope with the changes in the engine-out emissions, as the CO emissions were slightly over the Euro 5b emissions limit. NO_X emissions were reduced in the urban phase of the RDE, possibly due to the charge cooling effects of *n*BuOH reducing the in-cylinder temperature. However, in the motorway phase, the NO_X emissions increased relative to diesel due to lower EGR rates and higher in-cylinder temperatures. The engine-out PN emissions in the urban and rural phases of the test cycle were half those of diesel upon the addition of 10% *n*BuOH, and the motorway phase emissions were reduced by 40% [30]. The addition of *n*BuOH reduced the fuel consumption during the RDE by around 10%, even with the lower energy content of *n*BuOH relative to diesel. The successful use of *n*BuOH blended with diesel in on-road

vehicles shows that there is potential to use diesel blends containing biofuels other than biodiesel as drop-in fuels.

It is clear that further studies are needed into how advanced biofuel blends would perform during transient operation and in real-world applications. The research presented in this paper investigates the real-world driving emissions and performance of tailored three-component butyl blends with diesel in a Euro 6 hybrid vehicle, where the fuel blends were formulated to meet selected physical property limits [31]. The aim of this study was to assess the influence of the chosen butyl blend composition on the regulated emissions from a Euro 6 diesel hybrid vehicle, with a particular focus on the cold start emissions during RDE tests.

2. Materials and Methods

2.1. Test Vehicle

The vehicle used in this study was a 2018 Mercedes C300h. This is a Euro 6b-emission-compliant diesel NOVC hybrid vehicle with a twin turbocharged, common-rail direct injection compression ignition engine. The vehicle specification and after-treatment technologies are summarised in Table 1. The vehicle also has an EGR system as part of the emissions control set-up.

Table 1. Test vehicle specification.

Item	Detail
Model Year	2015
Year of Registration	2018
Engine Model	OM651 DE22 LA
Number of Cylinders	4 in-line
Displacement (cm^3)	2143
Maximum Power (kW)	150
Maximum Torque (Nm)	750
Transmission	7-speed automatic
Electric Motor Power (kW)	20
Hybrid Battery Capacity (kWh)	0.7
After-treatment Systems	DOC, DPF, SCR
Type Approval Test	NEDC
Approximate Mileage before Testing (km)	150,000
Curb Weight (kg)	1765

Prior to testing, a second complete exhaust system equipped with thermocouples and sample probes was installed on the vehicle, replacing the exhaust and after-treatment system the vehicle was supplied with, as shown in Figure 1. The second exhaust system was around 6 months old and had been used for less than 16,000 km [31]. The SCR system also had an ammonia slip catalyst (ASC) to remove ammonia. The original Mercedes exhaust sensors were installed into the fitted exhaust. The fuels were tested in the vehicle without any changes to the fuel system or engine control parameters.

2.2. Test Route

An RDE-compliant route was developed around the city of Leeds, UK, as shown in Figure 2. To ensure that the correct distances were attained for each phase of the RDE, some test sections of the route were repeated. The urban, rural, and motorway sections are determined by vehicle speed and not by GPS location. Hence, the required distances for the urban and rural sections can be achieved by repeating loops within the appropriate speed limits. The speed ranges for the urban, rural, and motorway sections are 0–60 km/h,

60–90 km/h, and >90 km/h, respectively. An example vehicle speed profile of the test route is shown in Figure 3. The details of the route are summarised in Table 2.

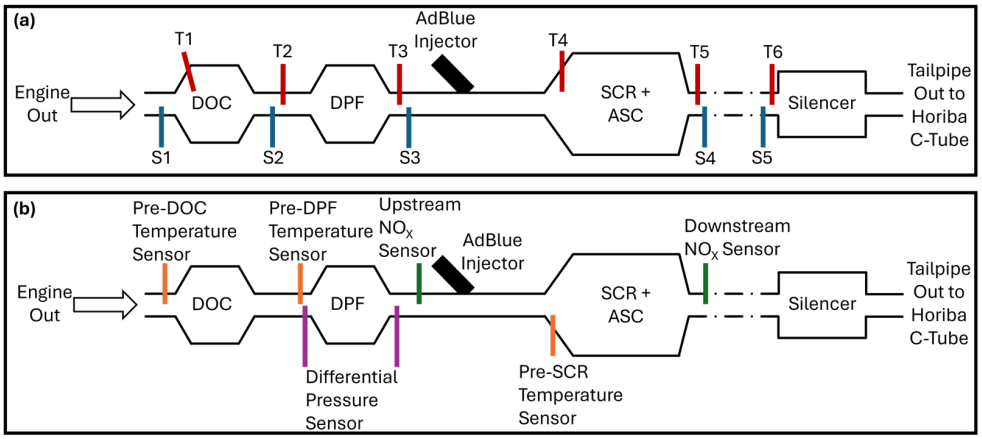

Figure 1. Schematic of exhaust after-treatment system and (**a**) additional k-type thermocouples (T) and sample probes (S). (**b**) The locations of the Mercedes sensors.

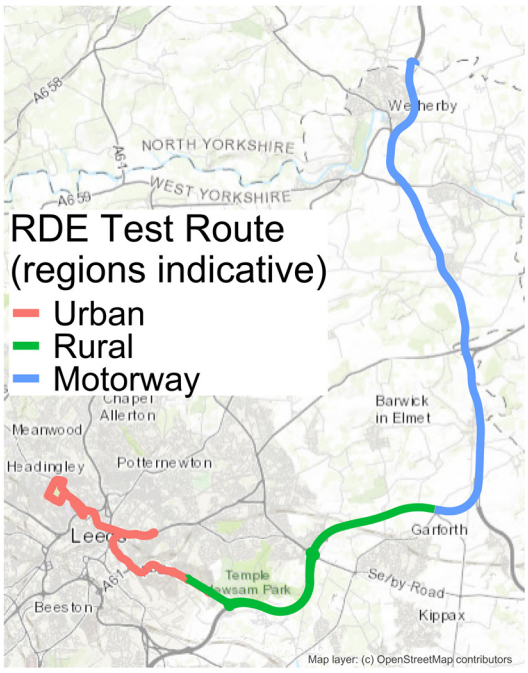

Figure 2. RDE test route with approximate sections of urban, rural and motorway phases in Leeds, UK.

Table 2. RDE test route parameters.

Description (Units)	Value
Total Trip Distance (km)	97.2
Urban Distance Share (%)	31.5–37.7
Rural Distance Share (%)	29–35.6
Motorway Distance Share (%)	29.6–35.2
Urban Speed Range (km/h)	0–60
Rural Speed Range (km/h)	60–90
Motorway Speed Range (km/h)	>90
Average Test Duration	1 h 54 min
Altitude Range (m)	24–103
Cumulative Elevation Gain (m/100 km)	563

The RDE tests conducted for this study were cold start tests. The vehicle was stored in the University of Leeds Research Vehicle garage from the end of the day until the next cold start test. It was left to sit in ambient conditions for around 18 h with no external cooling. The engine coolant at the start of the test was at the same temperature as the ambient surroundings prior to starting the RDE test.

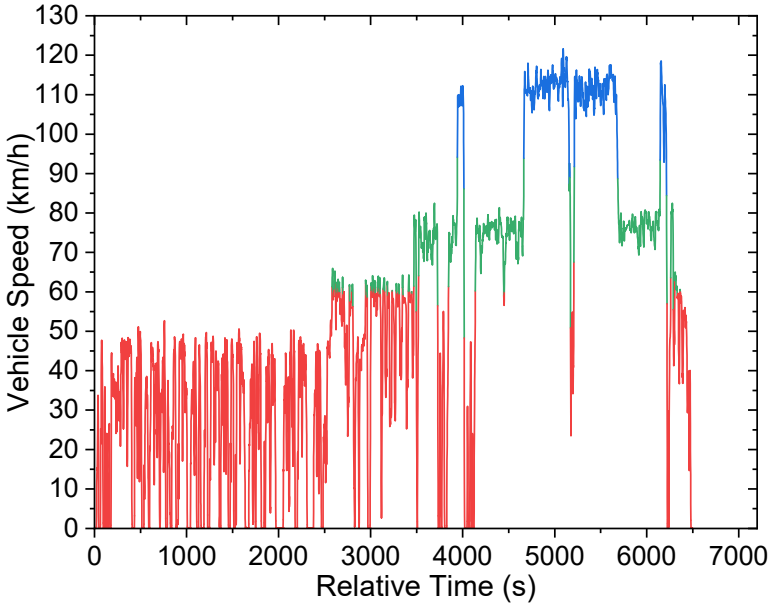

Figure 3. Example RDE test route vehicle speed profile from D100 trip 1. Red sections indicate regions that would contribute to the urban driving, green sections indicate the rural contributions, and blue the motorway contributions.

2.3. On-Board Equipment and Analysers

The vehicle was equipped with a Horiba OBS-ONE gas analyser (GS) and a particle number (PN) unit connected to a C-tube exhaust flow tube. The C-tube has two sample probes connected to the transfer lines for PN and GS units, respectively, pitot tubes, and a thermocouple. The GS had a heated transfer line at 180 °C, and the PN unit had transfer line held at 25 °C. The transfer lines were routed out of the vehicle through a removable vent and then under the vehicle to connect to the C-tube. The tailpipe of the vehicle was modified after the silencer to give a straight connection to the silicon Samco 90° connector, which connected the tailpipe and the C-tube, which itself was secured to the rear bumper of the vehicle as shown in Figure 4. The two analysers were secured in the boot of the vehicle and were powered using additional onboard batteries. The PN unit measured solid particles with aerodynamic diameters of 23–1000 nm, as required for Euro 6 [26]. The measurement techniques and calibrated ranges for each analyte are summarised in Table 3. A Horiba weather station was mounted to the rear pillar of the vehicle to measure ambient temperature and relative humidity. The OBS-ONE logged data at 10 Hz.

Engine control unit (ECU) parameters were logged using a Rebel LT logger (Influx Technologies, Bedford, UK), with the channels logged and the frequencies summarised in Supplementary Materials Table S1. These channels included engine speed (revolutions per minute (rpm)), engine coolant temperature, and pre- and post-SCR NO_X sensors. Most channels were logged at 1 Hz, with some data logged at higher frequencies due to their rapid fluctuations, such as fuel injection mass, and some at a lower frequency due to their slow change, such as DPF fill level. An additional onboard Gasmet DX4000 Fourier Transform Infrared (FTIR) spectrometer (Gasmet Technologies Ltd., Northampton, UK) and sample handling pump also contributed to the total vehicle mass. The data from

the FTIR measurements will be included in future publications. All pieces of equipment were powered using onboard batteries, with a separate set connected to the OBS-ONE. All other equipment was powered using an inverter connected to batteries to give 240 V mains equivalent electricity. The total onboard equipment weight, including batteries and inverter, was around 300 kg.

Figure 4. Installation of OBS-ONE and C-tube in the Mercedes C300h.

Table 3. Measurement techniques and calibration ranges of the OBS-ONE system [32,33].

Emission	Measurement Technique	Calibrated Range
CO	Non-Dispersive Infrared	0–10 vol%
CO_2		0–20 vol%
NO_X	Chemiluminescence	0–3000 ppm
PN (23–1000 nm)	Condensation Particle Counter—Isopropanol Working Fluid	0–5 × 107 #/cm^3
Exhaust Flow Rate	Pitot Flow Metre	0.3–10 m^3/min

2.4. Fuel Blend Preparation

The fuel blends were prepared in 20 L batches, using splash blending methods. The required volumes of the fuel components were added to the fuel drums in order of the least to most volatile, sealing the drum between additions to ensure there were minimal losses of fuel components. The drums were then shaken for one minute. The tolerance of the blend production was 1% to account for the errors on the measuring cylinders. The blends were prepared at least 48 h in advance and were shaken again before being used to fuel the vehicle.

The fuel blends tested (Table 4) were selected as they had shown promising performance and emissions when tested in a single-cylinder engine and were found to be compatible with the materials used in the fuel delivery system [23]. The ratios of the butyl components in the three-component blends and the blend-to-diesel ratio are shown in Table 4. This work aims to investigate the influence of the fuel blends on the emissions and performance of a Euro 6-compliant vehicle to determine if they can be used as drop-in fuels. Unlike the genset, the Mercedes C300h incorporates an ECU and after-treatment systems. The diesel (D100) used was a summer-grade EN 590-compliant diesel with 7 vol%

biodiesel (Tate Oil, Otley, UK). Purities of the biofuel components used to produce the representative alcoholysis mixtures were as follows: *n*BL ($C_9H_{16}O_3$) (98%, Fisher Scientific, Loughborough, UK), DNBE ($C_8H_{18}O$) (99+%, Fisher Scientific), and *n*BuOH (C_4H_9OH) (99% extra pure, Fisher Scientific). The pure components used in the butyl blends were not explicitly biobased as they were purchased high-purity chemicals, but they are representative of mixtures that could be produced from the alcoholysis of lignocellulosic biomass feedstocks [18,19,34,35]. The key physical properties of the fuel components are summarised in Table 5. These properties have been measured where possible, and those which could not be measured have either been calculated or use values taken from the literature [16,23,31].

Table 4. Fuel blends tested with values from [23].

Blend	Diesel:Biofuel Ratio (vol%)	*n*BL:DNBE:*n*BuOH Ratio (vol%)	Density at 15 °C (kg/m^3)	Calculated Lower Heating Value (MJ/kg)
D100	100:0	0	835	42.7
D90Bu10 – 65:30:5	90:10	65:30:5	843	41.4
D90Bu10 – 85:10:5	90:10	85:10:5	847	41.1
D75Bu25 – 85:10:5	75:25		863	38.8

Table 5. Fuel component physical properties.

Fuel Component	Density at 15 °C (kg/m^3) [a]	Kinematic Viscosity at 40 °C (mm^2/s) [a]	Derived Cetane Number (DCN) [c]	Heat Capacity (J/kg K) [d]	Lower Heating Value (MJ/kg) [f]	Boiling Point (°C) [g]
EN 590 Limits [22]	820–845	2.00–4.50	>51	None specified	None specified	None specified
BS 2869–2022 Limits [36]	>820	2.00–5.00	>45	None specified	None specified	None specified
Diesel	835 [b]	2.00–4.50 [h]	51 [h]	-	42.7 [h]	160–360 [h]
*n*BL	973	2.017	14	1962 [e]	27.4	232
DNBE	768	0.736	100–115	2135	38.3	142
*n*BuOH	811	2.261	12–16	2401	33.1	117

[a] Measured by an Anton Paar SVM3000, [b] measured following ISO 3838 [37], [c] from [38], [d] from [39], [e] from [40], [f] from [21,41–44], [g] from [39]. [h] These are typical diesel values.

When changing the fuel blends, the previous fuel used was drained from the vehicle by connecting a fuel pump to the inlet of the fuel swirler pot. This drained the fuel tank and the lines up to the fuel swirler pot. This portion of the fuel system was then flushed twice with 3 L of the new fuel blend being used, being drained after each 3 L portion. The fuel tank was then filled with the test fuel blend and pumped until the fuel was drawn to the swirler. This line was then connected to the swirler pot, and the vehicle was driven for around 20 km to use up the fuel that was in the section from the fuel swirler to the injectors and in the common rail.

2.5. Data Processing

The 10 Hz OBS-ONE data was processed using the accompanying Horiba post-processing software (version 4.8.2) following the RDE Package 4 methodology [45]. As part of this analysis, 1 Hz data was generated using the average of the 10 Hz data. The processing gave the emissions factors for each RDE phase and the total RDE, along with the fuel economy determined using a carbon balance method. A CO_2 moving average window (MAW) method was used to ensure test conformity and compliance. The CO_2 window was created using half the CO_2 emitted for each phase of the WLTP. A WLTP test was conducted by Horiba MIRA to acquire the required CO_2 emissions data since the vehicle was type approved using the NEDC test.

The 1 Hz data from all data loggers was time aligned using the correlation method in the pem.utils R package (version 0.3.0.8) [46,47]. The OBS data was used as the base

data set with the Rebel LT logger aligned using the exhaust pressure sensor data and the OBS-ONE exhaust mass flow measurement. The temperature data presented in Section 3 was data recorded from the vehicle's temperature sensors.

The fuel economy from each RDE test was calculated by the Horiba software (version 4.8.2) using a carbon balance methodology based on the emissions measured by the OBS-ONE, the elemental composition of the fuel blends, and the density of the fuel [48].

The results presented in this work are from three cold start RDE tests for each blend. These did not include DPF regeneration, as this did not occur when using each fuel.

3. Results and Discussion

The error bars shown on each plot represent one standard deviation across the three tests conducted for each fuel blend. It is possible that the mass of the loaded vehicle may have influenced the amount of time it spent being propelled by the electric motor compared to when the vehicle is not laden. However, the vehicle's mass throughout the test programme varied by no more than 2%, with any changes being due to fuel being consumed and changes in passenger weights. The same driver and test equipment were on board for all tests. Therefore, we expect little influence of the vehicle's mass when comparing the emissions from each fuel.

Similarly, more power and torque are needed to accelerate a heavier vehicle. Hence, the electric motor often acts in a boosting function in combination with the ICE to accelerate the vehicle. During low load running, particularly during the urban phase of the RDE or during cruising at constant speed on the motorway, the ICE would turn off and the vehicle would be propelled solely by the electric motor. There were common places where this occurred on most tests. For example, in one of the repeated sections in the urban phase of the RDE, the engine would turn off in most tests, indicating full use of the electric motor. When the engine is off, the exhaust and after-treatment systems cool, which can increase the time taken until they reach light-off temperature, or they can cool to below their light-off temperatures. Any cooling of the catalysts can also reduce their activity, which can result in increased emissions after the reignition of the ICE [29,49]. We would therefore expect variations in these factors to cause some variability in emissions between tests.

3.1. Fuel Economy and Vehicle Drivability

When using the biofuel blends, there were no discernible differences in drivability during the RDE tests. There were no issues with vehicle start-up or during ignition events when switching from electric to ICE driving modes. The engine and ECU were able to cope with the additional oxygen content in the fuel, as well as changes in density, and cetane number (CN) due to the presence of the biofuel components. The derived CN (DCN) of *n*BL is 14.4 and *n*BuOH is 12, i.e., significantly lower than that of diesel (Table 5) [38].

Fuel economy was defined as the number of litres of fuel required to complete 100 km, as required by the RDE testing methodology. The average fuel economy values for the three cold start RDE tests and the relative changes are displayed in

The fuel economy of each fuel tested showed a maximum of a 5% increase compared to diesel in the vehicle tests when used as a drop-in fuel. In fact, the reduction in the fuel's energy content has not had a significant impact on the vehicle's fuel economy. D75Bu25 – 85/10/5 has a lower heating value (LHV) which is 9% lower than that of diesel (Table 4) but only showed a 3% increase in fuel consumption. This difference in the change in fuel consumption, relative to diesel, compared to the reductions in lower heating value relative to diesel is likely due to the butyl blends having a slightly higher density than diesel (Table 4). The increased density will result in a slightly greater mass of fuel being injected, compensating for the reduced LHV. Therefore, these oxygenated biofuels can

be blended to a significant fraction with diesel without a significant deterioration in fuel economy. Figure 5.

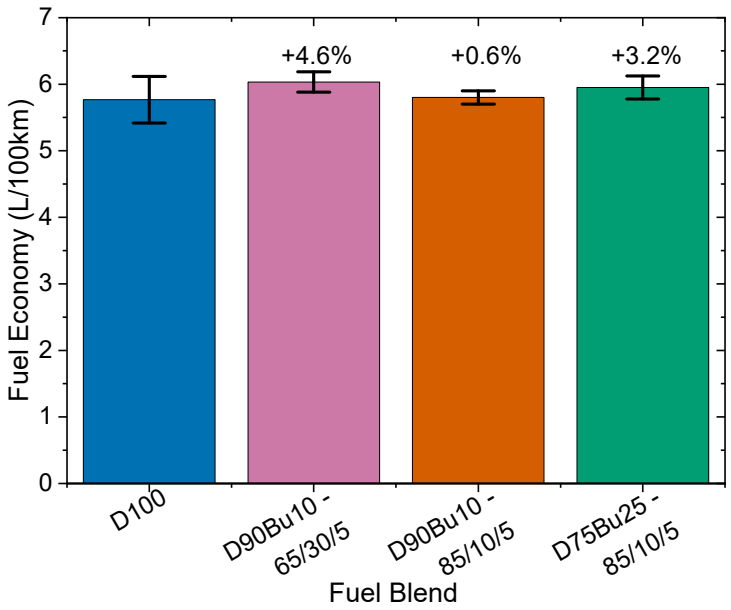

Figure 5. Comparison of C300h fuel economy for each fuel blend tested.

3.2. Influence of Biofuel Blends on Cold Start Emissions

The cold start period of the RDE is defined as the duration of the test before the coolant reaches 70 °C or 300 s if the coolant does not reach 70 °C before this. During this time, the DOC and SCR did not reach their light-off temperatures, and the SCR reductant, AdBlue, is not being injected.

Typically, cold starts are likely to occur in urban settings due to commuting; thus, reducing the local emissions in these settings would improve local air quality, along with associated negative public health impacts. Therefore, the impacts of any new fuel on the emissions in these periods must be understood. In addition, future emissions regulations, including Euro 7, will be putting a larger emphasis on cold start emissions, with vehicles having to meet set limits for hot and cold start RDE tests [50].

The changes in the total cold start emissions of all pollutants between the fuel blends were not statistically significant due to the high variability in the separate RDE test results. However, it will become evident from the following results sections and in the cumulative cold start emissions of CO, NO_X, and PN, as shown in Figures 6, 8 and 12, respectively, that there is an influence of the fuel blend on the cold start emissions when the average emissions are compared. The high variability in RDE testing is something that is difficult to overcome as no two tests will ever be the same. The standard deviations are used as an indication of the variance of the tests. There are a variety of reasons why the emissions during the cold start period were variable. These include the following:

- Different amounts of time spent during each test with the engine-off, due to switching between electric only and combined ICE and electric motor driving.
- Varying distances covered during the initial five minutes of each test due to differing traffic conditions. These distances ranged from 1.16 to 2.09 km. Therefore, depending on the distance covered, different junctions would have been included within the cold start period leading to differences in total gradients and traffic signal waits and accelerations. These would result in different emissions profiles due to different loads on the powertrain.

- Different traffic conditions, resulting in different driver responses to other road users and traffic. Whilst the same driver conducted each test to reduce the influence of driving style, there were still differences in the nature of the traffic from day to day and from test to test.
- Different ambient temperatures, as these would affect combustion due to air density changes as well as changes to exhaust temperatures and catalyst activation.

3.2.1. Influence of Biofuel Blends on Cold Start CO Emissions

Figure 6 shows that the two Bu10 blends, on average, reduced the CO emissions relative to diesel, and D75Bu25 – 85/10/5 increased CO emissions relative to diesel. In addition, it is evident that increasing the *n*BL fraction in the biofuel blend and total biofuel blend fraction of the fuel increased the CO emission relative to diesel. The CO emissions were reduced by 52% and 22% relative to diesel for D90Bu10 – 65/30/5 and D90Bu10 – 85/10/5, respectively, whereas they increased by 25% relative to diesel with D75Bu25 – 85/10/5. Increases in engine-out CO emissions relative to diesel were observed by Wiseman et al. [23] when testing these fuel blends under steady-state conditions in a genset single cylinder diesel engine. Whilst those emissions were not cold start emissions, the increases in the genset showed that even with oxygen in the fuel, there could still be an increase in engine-out CO emissions relative to a diesel baseline.

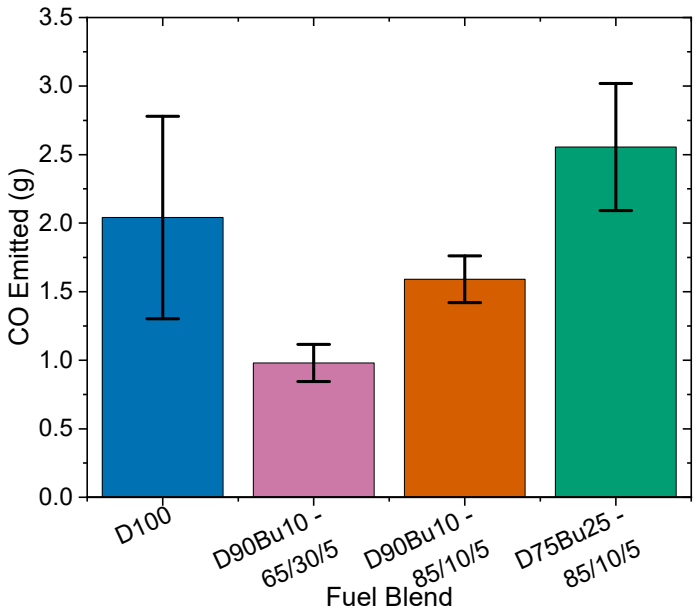

Figure 6. Average cumulative cold start CO emissions during the first 300 s when using each of the fuels tested.

Figure 7 shows examples of the CO concentration, the temperature before the DOC, and the engine speed for selected trips. In the test with D90Bu10 – 65/30/5 (Figure 7b), the pre-DOC temperature reaches the 200 °C typical light-off temperature later than when running the other fuels. However, the total CO emitted during the cold start when running D90Bu10 – 65/30/5 was lower than that when running the other fuels (Figure 6). This is indicative that the fuel is promoting complete combustion, producing less CO than the other fuels. One possible reason for the lower CO may be the higher fraction of DNBE present in the blend compared to the other Bu10 blend. DNBE has a DCN of 100–115 (Table 5), which is the highest of all the major fuel components. Higher DNBE fractions may therefore enhance combustion by reducing the ignition delay, ensuring there is sufficient time for complete combustion [38]. Figure 7d shows that the first 74 s of the test when using

D75Bu25 – 85/10/5 had high concentrations of exhaust CO, even during the period where the engine is idling (where the engine speed is around 730 rpm). When running with blend D90Bu10 – 65/30/5 (Figure 7b), where there is also a period of idling at the start of the test, the CO concentration is lower than when running with D75Bu25 – 85/10/5. During a cold start, more fuel is injected to decrease the time taken to raise the temperatures, and since the injectors and fuel are cold, fuel viscosity is increased; thus, the fuel vapourisation rate is reduced [51]. Since *n*BL has a high boiling point, as the fraction of it increases in the butyl blends, the fuel atomisation during cold start would be worse, resulting in less complete combustion and higher CO emissions. The low DCN of *n*BL will also contribute to the increased CO emissions at high blend fractions, as there would be a longer ignition delay and less time for complete combustion [38].

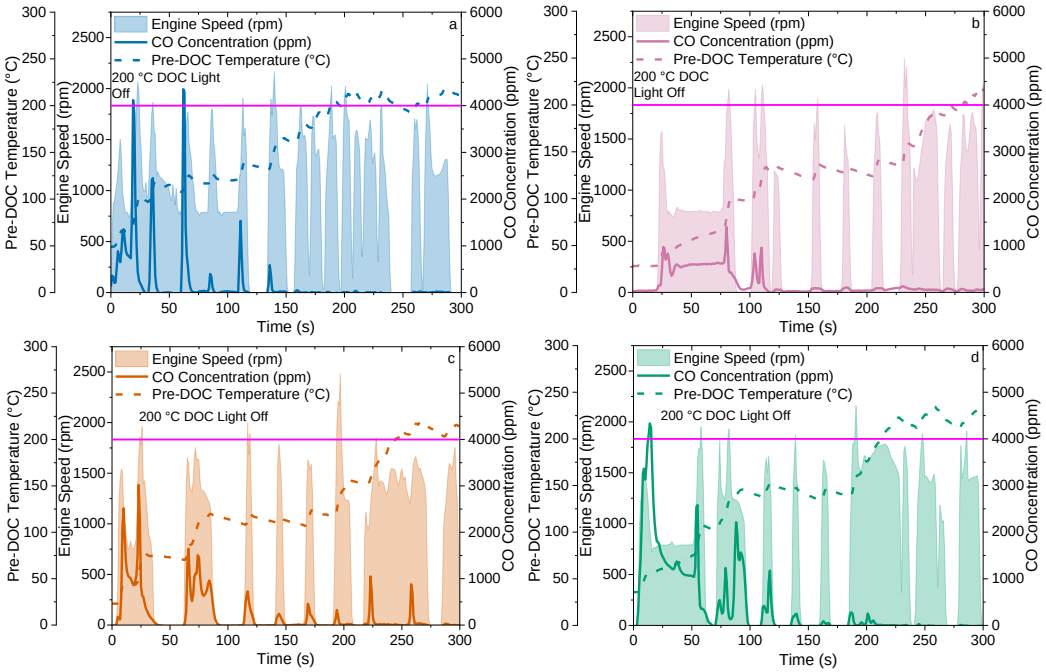

Figure 7. CO concentrations, engine speed, and pre-DOC temperatures during the cold start period for RDE tests using the different fuels: (**a**) D100 trip 3, (**b**) D90Bu10 – 65/30/5 trip 1, (**c**) D90Bu10 – 85/10/5 trip 2, and (**d**) D75Bu25 – 85/10/5 trip 3. The horizontal purple line in each figure indicates the DOC light off temperature.

The potential causes of variability between trip CO emissions and the potential influence of the hybrid operation were investigated using the number of ICE reignitions and the total engine-off duration. No direct correlation between the total cold start CO emissions and the number of reignitions or the total cold start CO emission and total engine-off duration could be found. This data is therefore not reported here. The lack of correlation could be due to the complexity of the variables as they include different fuel blends, different distances covered, the number of traffic signals, the behaviour of other road users, and traffic levels, all within a fairly small sample size of 12. A high number of reignitions and long engine-off duration should produce lower cumulative CO emissions since, when the engine is off, no CO would be produced. However, in this case, the fuel blend seems to be an important factor as indicated in Figure 6, with the variability between trips caused by other on-road factors.

3.2.2. Influence of Biofuel Blends on Cold Start NO_X Emissions

Figure 8 shows that average cumulative NO_X emissions during the cold start period (the first 300 s of the trips) reduce relative to diesel upon addition of the biofuel blends.

The changes in NO_X emissions were not statistically significant due to the high variability between the repeat tests. The cold start NO_X emissions when using the biofuel blends were within one standard deviation of the diesel baseline, as indicated by the error bars. During the cold start period, there is no active removal of NO_X as the SCR has not reached light-off temperature, and typically EGR is not operational during cold start periods. Therefore, any reductions in NO_X emissions were caused by changes to the fuel and variations in the engine operation during the cold start period. The NO_X emitted is likely to be dominated by thermal NO_X, so any changes in combustion temperatures due to the fuel blends would result in changes in NO_X emissions [30,52]. The average NO_X emissions reduced relative to diesel by 15%, 16%, and 26% for D90Bu10 – 65/30/5, D90Bu10 – 85/10/5, and D75Bu25 – 85/10/5, respectively. Similarly, Antonetti et al. [21] observed slight reductions in NO_X emissions relative to diesel with increasing biofuel fraction from 10 to 30 vol% for a fixed butyl blend of 70 wt% *n*BuOH, 20 wt% DNBE, and 10 wt% *n*BL, with greater reductions at lower engine speeds, although the impact of the fuel blend composition could not be determined.

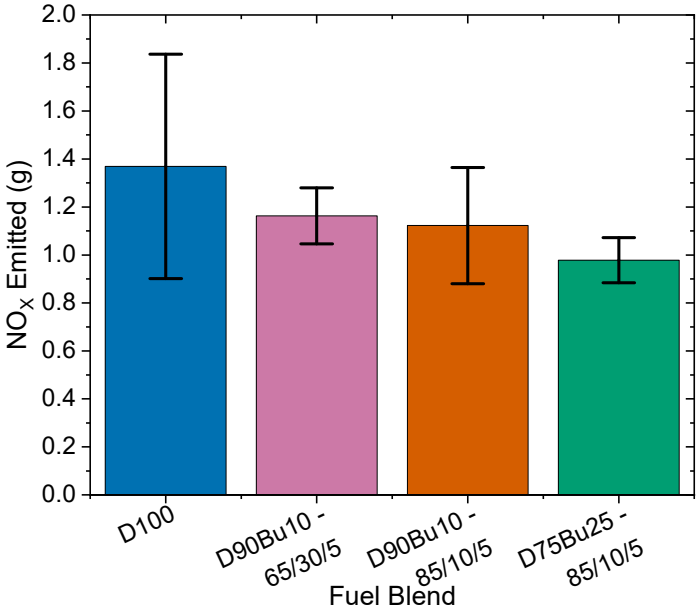

Figure 8. Average cumulative cold start NO_X emissions during the first 300 s when using each of the fuels tested.

Figure 9 shows that the NO_X emissions spike at the points of acceleration, where the engine speed rapidly rises. This would be expected during the cold start period, as the engine typically runs richer to increase its temperature, resulting in more NO_X being produced. The magnitude of the peak NO_X emissions was variable, as were the durations of periods of sustained high NO_X emissions, and this is indicative of the variability during RDE testing. There is limited evidence of the impact of the biofuel blends on the combustion temperatures as the exhaust temperatures pre-turbocharger for the fuels were all similar, as shown in Figure 10. The impact on the heat release rate when using the biofuel blends was not measured. However, the peak heat release rate may have been delayed, resulting in lower peak temperatures close to top dead centre and thus lower engine-out NO_X emissions, as a delay in peak heat release was observed when these fuels were tested in a genset by Wiseman et al. [23].

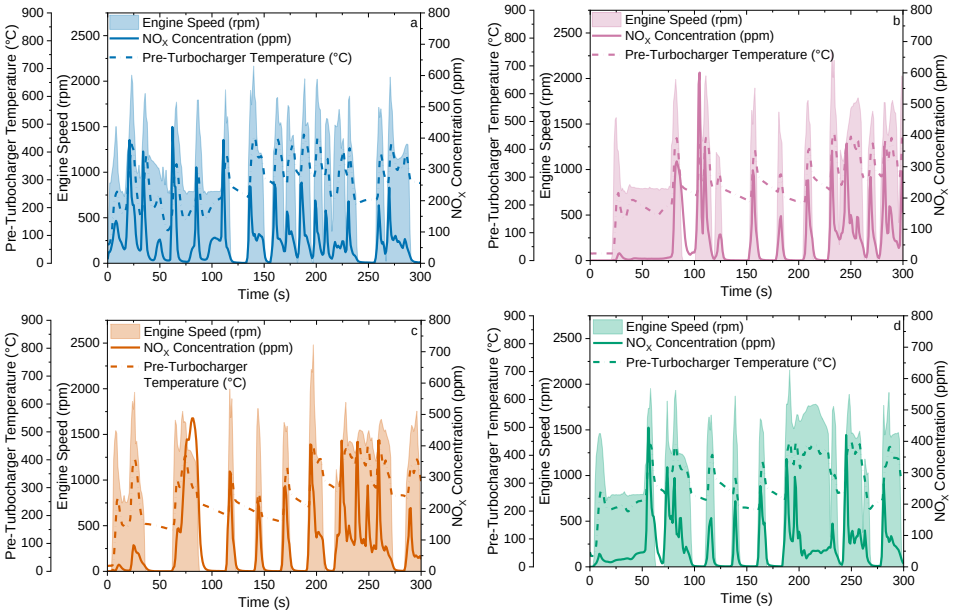

Figure 9. NO_X concentrations, engine speed, and pre-turbocharger temperatures during the cold start period for RDE tests using the different fuels: (**a**) D100 trip 3, (**b**) D90Bu10 – 65/30/5 trip 1, (**c**) D90Bu10 – 85/10/5 trip 2, and (**d**) D75Bu25 – 85/10/5 trip 3.

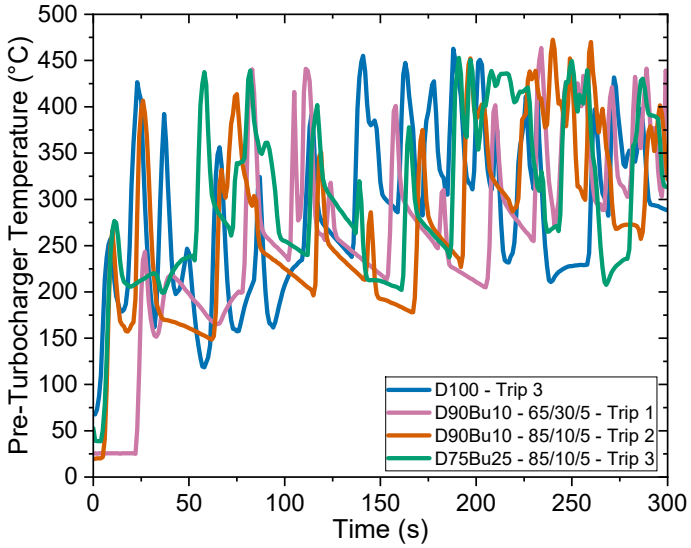

Figure 10. Comparison of the pre-turbocharger temperatures during the cold start period for the RDE tests of selected trips with each fuel. These are the same trips shown in Figure 9.

The number of reignitions and total engine-off duration were both found to have direct non-linear correlations with the total mass of NO_X emitted across all tests as shown in Figure 11. The R^2 values are 0.631 and 0.630 for the fits to the number of reignitions and the engine-off duration, respectively, indicating a good fit to the data for a sample size of 12. The higher number of reignitions coincide with longer engine-off durations; hence, the correlations are very similar. As expected, it can be seen that the longer the engine is off, the less NO_X is emitted. Typically, NO_X emissions spike (see Figure 9) as the vehicle is accelerating and the engine load increases. These spikes in NO_X emissions contribute a large proportion of the NO_X emissions during the cold start period (Figure 9). The variability in the engine-off duration contributes to the variability in the NO_X emissions, since the engine is not producing NO_X when the engine is off. Improving cold start emissions would be the target in order to improve air quality in urban areas, where most cold start trips occur, and the biofuel blends perform well in this regard.

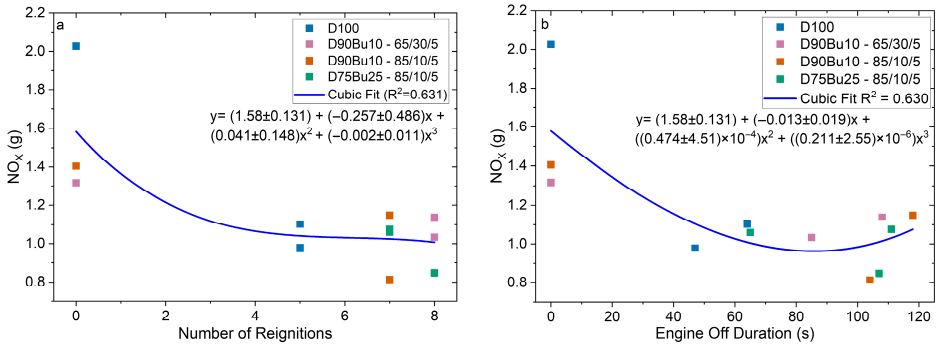

Figure 11. Influence of (**a**) the number of reignitions and (**b**) the engine-off duration on the NO_X emitted during the cold start period. The coefficients of the fitted cubic equation are given to three significant figures.

3.2.3. Influence of Biofuel Blends on Cold Start PN Emissions

The addition of the biofuel blends reduced the total PN emissions during the cold start period relative to diesel, as shown in Figure 12. When accounting for the standard deviations (error bars) in the PN emissions with each fuel, there is a relationship between the *n*BL and biofuel fraction and the reduction in PN. The error bars are large for D100 and D90Bu10 – 85/10/5 due to the cold start periods all being different for each test. Since the cold start is defined as a duration, there are many factors that can influence the PN emissions during the cold start period. Wiseman et al. [23], Frigo et al. [53], and Antonetti et al. [21] similarly observed reduced particulate emissions when testing butyl blends with diesel. They also observed that the reduction in particulates relative to diesel was correlated with the *n*BL fraction. One key reason is the net reduction in the fuel aromatic content when a fraction of the diesel volume is replaced by the biofuel blend, resulting in fewer particulate precursors being formed. Therefore, the higher the volume fraction of *n*BL and biofuel in the blend, the fewer solid particles were produced. Additionally, lower tailpipe PNs indicate lower engine-out emissions, as the DPF is constantly active and was assumed to have the same efficiency for all fuels.

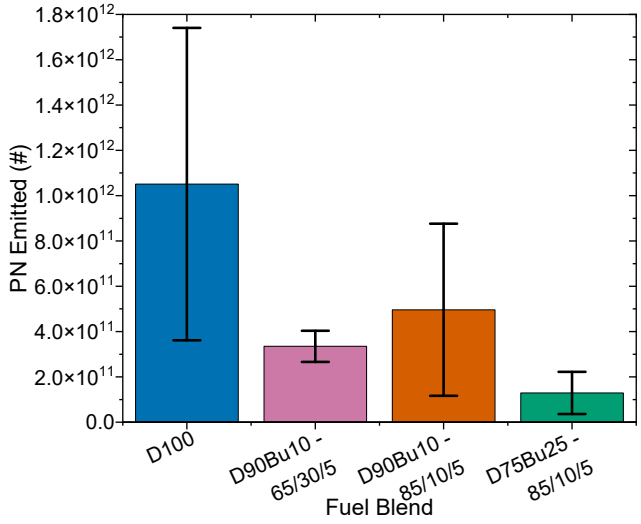

Figure 12. Average cumulative cold start PN emissions during the first 300 s when using each of the fuels tested.

Cold start PN emissions would typically account for a large fraction of the total emissions for a given trip, so any reduction in cold start emissions would be favourable from a local air quality perspective. The total trip cumulative PN emissions will be discussed

further in Section 3.4. Since the cold start PN emissions reduce with the addition of the butyl blends, their contribution to the cumulative emissions will also be observed to reduce.

Figure 13 shows that during the cold start, the large spikes of PN emissions are due to acceleration and reignition events of the engine, as when the engine speed drops to zero, the vehicle is either stationary or being driven by the electric motor only. For example, it can be seen in the diesel test (Figure 13a) that at 100–150 s, where there is an acceleration followed by engine off, ignition, and acceleration, there are two peaks in PN that follow the nature of the engine speed trace. However, as the engine warms up, the PN decreases, and even with rapid increases in engine speed, there were much smaller spikes in PN emissions. This happens for all the fuels, but at different times and with different orders of magnitude difference in PNs, as shown when comparing Figure 13a,d. No statistically significant correlations were found between the total PN emitted during the cold start and the number of reignitions or the total PN and the engine-off duration. This indicates that the use of the electric motor did not have a significant impact on the control of the tailpipe PN emissions. Therefore, it seems reasonable to conclude that the DPF is highly effective and can handle any changes in engine-out emissions when the engine reignites following the sole use of the electric motor using all four fuels tested. The number of reignitions and engine-off duration contribute to the variance represented by the error bars in Figure 12. The nature of the traffic and the traffic signal settings are likely to have had an impact on the variability between the tests. There are 14 sets of traffic signals between the start of the RDE test route and the furthest point reached within 5 min, any number of which could stop the flow of traffic. Some of these traffic signals are on a section of road with an uphill gradient, and whilst every effort was taken to accelerate steadily, the human influence of not being able to accelerate in an identical manner between each trip was likely to be a factor. However, overall, despite trip variability, there were indications of a stronger association between the fuel blend composition and the PN emissions, which is in agreement with the findings of Wiseman et al. [23], Frigo et al. [53], and Antonetti et al. [21].

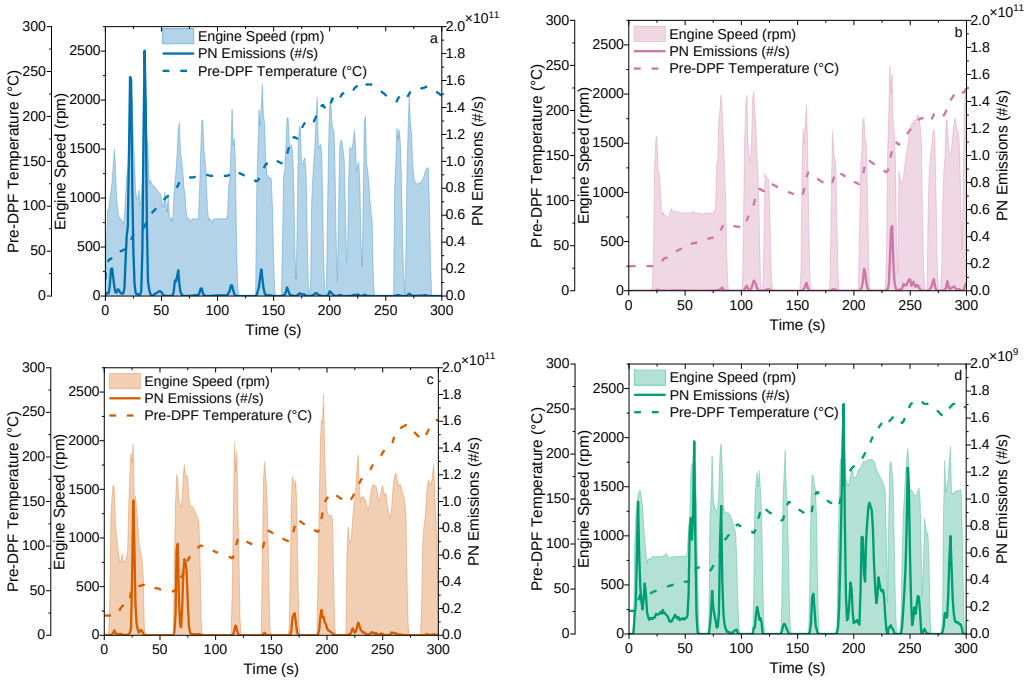

Figure 13. PN emissions, engine speed, and pre-DPF temperatures during the cold start period for RDE tests using the different fuels: (**a**) D100 trip 3, (**b**) D90Bu10 – 65/30/5 trip 1, (**c**) D90Bu10 – 85/10/5 trip 2, and (**d**) D75Bu25 – 85/10/5 trip 3. Note the scale for PN emissions on d is 100 times smaller for the PN concentration.

Reductions in PN emissions during cold starts would be beneficial for local air quality. Typically, the cold start periods for most journeys are in relatively densely populated urban areas, where reducing the exposure to particulate emissions could potentially improve both acute public health outcomes such as for respiratory and cardiovascular diseases, as well as the incidence of chronic diseases such as cancer and dementia [54]. The lower PN emissions therefore make the butyl blends an attractive alternative to diesel.

3.3. Influence of Biofuel Blends on Distance-Based CO Emission Factors for the Whole Trip

The distance-based CO emission factors for each of the RDE sections and the total emissions factors for the biofuel blends were lower than those of D100, as shown in Figure 14. The emissions were all below the Euro 6 limit of 500 mg/km.

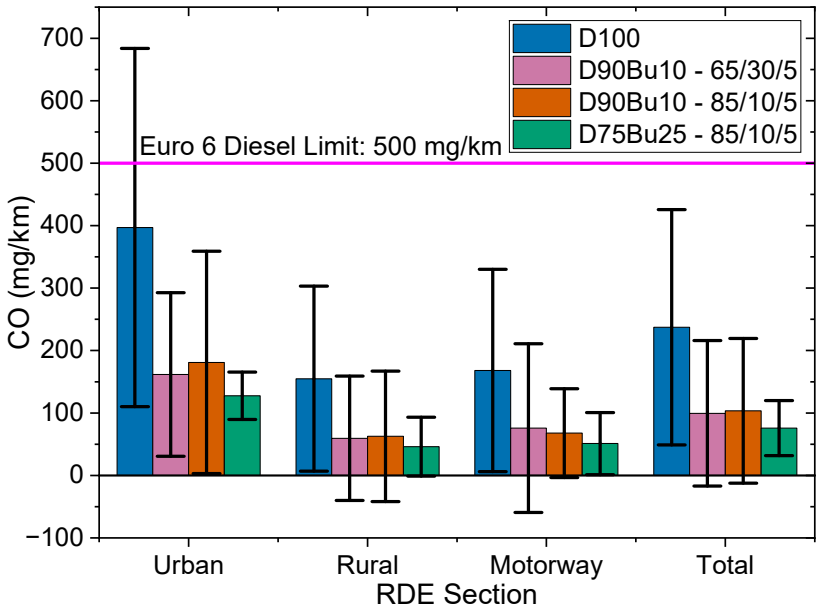

Figure 14. Comparison of CO emission factors from C300h for each RDE section with each fuel blend tested, and comparisons to the Euro 6 limit.

The whole-trip CO emission factors were reduced by 51%, 70%, and 72% relative to diesel, for D90Bu10 – 65/30/5, D90Bu10 – 85/10/5, and D75Bu25 – 85/10/5, respectively. The reductions for the CO emission factors in each section were similar to the total reductions when using D75Bu25 – 85/10/5, showing that the blends gave benefits at all engine loads and vehicle speeds. The large standard deviation of the three tests is an indication of the variance in the CO emissions with these fuels and with the measurement of the CO concentration. Although further testing is being considered to improve the accuracy of the uncertainty limits and/or better characterise variance, the observed trends still provide a reasonable indication of the influence of the fuels on the emissions. Although the changes in CO emission factors were not statistically significant at a 95% confidence level (mostly due to the large variability in CO emission factors during the diesel tests and a small sample size of three), the test data indicates reductions in the different RDE sections (Figure 14). The reduction in CO was related to the composition of biofuel blend fractions, as D75Bu25 – 85/10/5 had a greater reduction in tailpipe CO compared to the other blends for all RDE sections. Since all emissions were measured at the tailpipe, the emissions control from the DOC would require further testing to determine if it had operated at a constant efficiency with each fuel blend. It is likely that the addition of the biofuel blends had a direct influence on the CO formation during combustion, as Antonetti et al. [21] observed reductions in CO emissions when testing similar biofuel blends in a small engine. The reduction in CO

emission factors from the vehicle was likely due to the increased oxygen content in the fuel, combined with the high fuel injection pressure used in common rail diesel engines [55]. This is evident when comparing the changes in CO emissions from a single-cylinder engine, where the fuel injection pressure is around ten times lower than in the Mercedes (196 bar in the genset and 1988 bar in the Mercedes), and CO emission factors more than doubled for the high *n*BL blends compared to diesel [23]. The increased atomisation of the oxygenated biofuel blends will favour complete combustion, hence reducing the CO emission factors relative to diesel. During the cold start period, fuel atomisation may have contributed to the increased CO concentrations with the D75Bu25 – 85/10/5 blend, as the atomisation of D75Bu25 – 85/10/5 may have been worse than diesel due to its higher density (Table 4). Once the engine was up to temperature, the atomisation of the fuel would have improved, enabling the oxygenated biofuel compounds to contribute to reducing CO emissions.

3.4. Influence of Biofuel Blends on Distance-Based NO_X Emission Factors for the Whole Trip

The RDE for diesel and the biofuels are over the Euro 6 limit for NO_X (Figure 15). This is due to the limits being set for the WLTP laboratory-based test, which is not fully representative of real-world driving. Hence, the conformity factor (CF) was introduced. The applicable CF value for a pre-RDE vehicle is 2.1, resulting in a not-to-exceed (NTE) limit of 168 mg/km, as shown by the blue line in Figure 15 [25]. The total NO_X emission factor when using D75Bu25 – 85/10/5 exceeded the 168 mg/km limit, but it is within one standard deviation of it, demonstrating that it is possible to remain compliant with the emissions standard whilst running with D75Bu25 – 85/10/5. This, however, would require running multiple RDE tests for type approval in order to account for variability. Complying with the limit would result in the vehicle being eligible for free entry into emissions control zones where Euro 6 NO_X limits must be met. NO_X emission factors from the C300h increased relative to diesel upon the addition of the biofuel blends. The total NO_X emission factors increased by 13%, 12%, and 26% relative to diesel for D90Bu10 – 65/30/5, D90Bu10 – 85/10/5, and D75Bu25 – 85/10/5, respectively. The increases in NO_X emission factors were not statistically significant at a 95% confidence level, likely due to the inter-trip variability. The high variance in the motorway phase results for each fuel, indicated by the standard deviations of the three tests, are likely due to the high engine load and the greater variability of motorway traffic influencing acceleration, leading to variable NO_X emissions. The results in Figure 15 indicate that better NO_X control is required, especially for motorway driving where NO_X emission factors were highest for all fuel blends. The NO_X emissions in the rural and motorway phases increase with increasing nBL fraction and biofuel content. These increases occur when the engine and exhaust after-treatment system are up to temperature. In contrast, the cold start data (Figure 8) showed reduced NO_X emissions with increasing *n*BL and biofuel fraction, i.e., lower engine-out emissions. These contrasting results indicate that there is less effective removal of NO_X by the after-treatment systems for the biofuel blends over the whole trip. The addition of the biofuel blends to diesel and their use in this vehicle could result in compliance with the emissions limits when accounting for the variability. However, the increases in NOx for the biofuel blends do indicate that more effective emissions control strategies may be needed for these blends, since the emissions control strategy was likely to have been optimised around using diesel as a fuel.

During the urban phase of the RDE, there is a set of traffic signals where the wait time could be up to two minutes, which is below the maximum 5 min allowed time for a single stop during the urban phase. However, this stop would often be with the engine off, so the catalysts and exhaust would have cooled down. Throughout many of the tests with the different fuel blends, the pre-SCR temperature dropped below 150 °C, the temperature

at which AdBlue is injected in this vehicle. Therefore, the SCR system is likely to reduce in activity as it cools, and it would likely not be active during the periods where the temperatures fall below 150 °C. The influence of these individual cooling events on the tailpipe emissions upon engine reignition require further investigation [29,49,56].

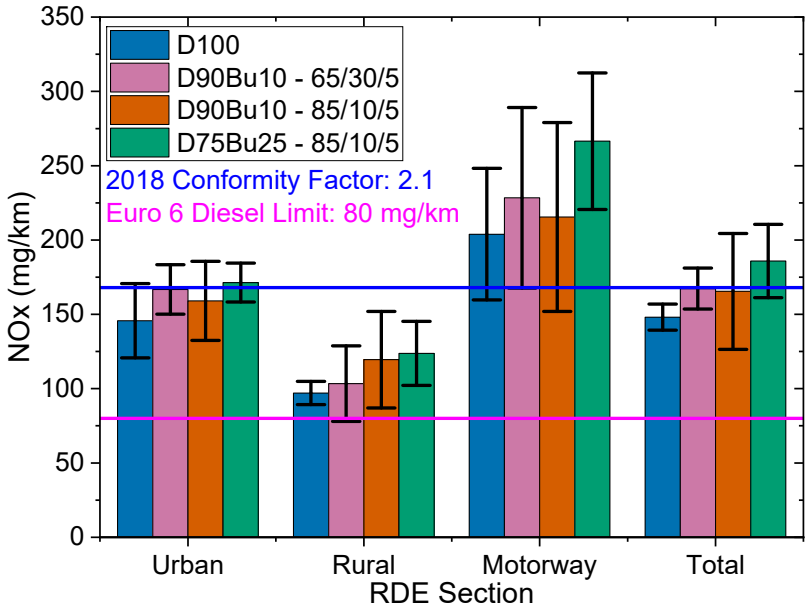

Figure 15. Comparison of NO_X emission factors from C300h for each RDE section with each fuel blend tested, and comparisons to the Euro 6 limit and the 2018 CF.

The increases in NO_X align with reductions in PN and CO. However, it is likely that rather than there being the expected soot–NO_X trade off due to differences in combustion characteristics, there is an influence of the SCR efficiency on total-trip NOx emissions [57]. Using the pre- and post-SCR NO_X sensors, the total mass of NO_X emitted as measured by these sensors could be determined. The fraction of total-trip NO_X removed by the SCR for each trip has been calculated by taking the difference between the two sensors (Figure 16). The reduction in the SCR efficiency can be seen in Figures 16 and 17, as the pre-SCR sensor measured similar total-trip NO_X emissions, with a slight reduction for D90Bu10 – 85/10/5 and D75Bu25 – 85/10/5 compared to D100. The NO_X sensors only measure the NO_X concentration when the sensors are up to temperature, which can be up to 20 min into the test, accounting for some of the variance in the total amounts of NO_X measured during the RDE trips. However, during these measurements, the SCR would have reached the light-off temperature, and AdBlue was being injected. The OBS-ONE was measuring tailpipe NO_X emissions throughout the whole test, which accounts for some of the differences in the presented values, along with differences in accuracy of the onboard sensors and OBS-ONE. The results are indicative of a decline in SCR efficiency when using the biofuel blends relative to D100, and this is supported by the increase in tailpipe NO_X emissions measured by the OBS-ONE when using the biofuel blends compared to D100. The fraction of NO_X converted by the SCR is shown to have a step change with each biofuel blend tested, rather than a gradual deactivation. To confirm that the deactivation was not permanent, one RDE was conducted with D100 after the final D75Bu25 – 85/10/5 test. The NO_X conversion for that D100 trip was at 63%. Whilst this is lower than the two tests at the start of the campaign with conversions of 68%, it is above the average conversion when running D75Bu25 – 85/10/5 of 58%. Therefore, the SCR conversion was recovering following any potential deactivation after running with the biofuel blends.

Further testing would be needed to investigate the long-term effects of the biofuel blends on the SCR efficiency.

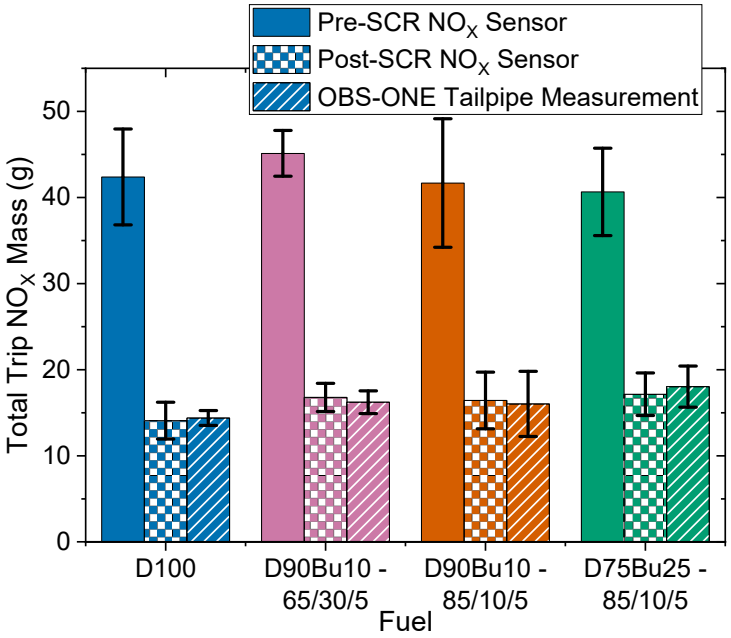

Figure 16. Average total mass of NO_X emitted as measured with the vehicle's own NO_X sensors pre- and post-SCR, and the tailpipe measurement using the OBS-ONE.

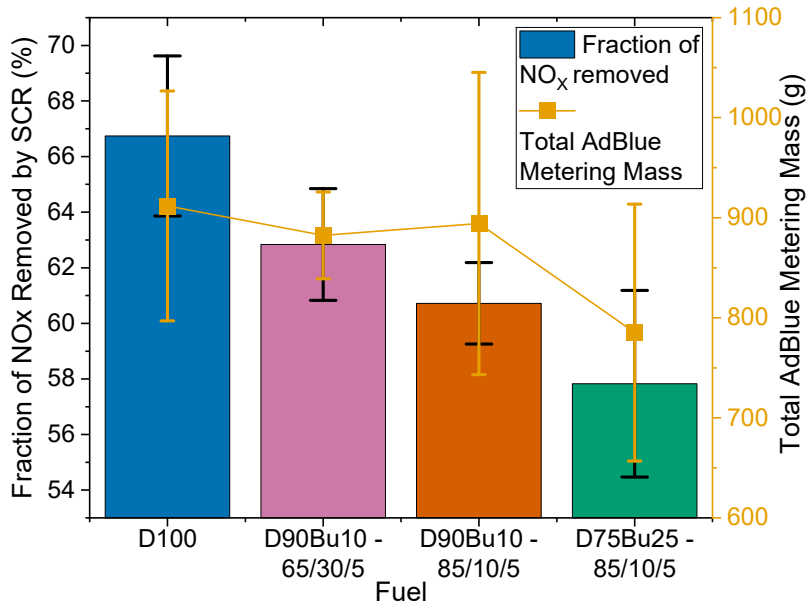

Figure 17. Fraction of NO_X removed when comparing the pre- and post-SCR NO_X sensors with the average total mass of AdBlue injected for the RDE tests with each fuel.

The amount of AdBlue injected changed based on the measured pre-SCR NO_X concentration (Figure 16), which was lower for most of the tests with the biofuel blends. This gives further indication that the SCR efficiency reduced, since the same fraction of NO_X could not be removed by the SCR with the butyl blends as with D100 (Figure 17). The results indicate the potential influence of NOx speciation, or of emissions of other species such as hydrocarbons, on the SCR catalyst efficiency [58,59]. The vehicle ECU and SCR control system would have deemed the quantity of AdBlue to be sufficient for the NO_X emissions for that trip as there were no engine management light warnings during the tests.

Therefore, the vehicle was not exceeding its own preset NO_X limits during these trips, but if further SCR deactivation occurred, those limits may be exceeded. The reduced injected quantity of AdBlue for the biofuel blend tests compared to D100 tests with similar levels of total pre-SCR NO_X indicates further analysis of transient pre-SCR and post-SCR NO_X concentrations, exhaust flow rates, and temperatures are needed as these are key parameters for the closed-loop SCR control strategy that determines the injected AdBlue quantity.

The exhaust gas temperatures did not significantly increase with the addition of the biofuel relative to when running diesel, as shown in Figure 10. This is, therefore, not the likely reason for increases in the tailpipe NOx when using the biofuel blends. The SCR system, in conjunction with the DOC to oxidise NO to NO_2, would have been designed using diesel exhaust compositions and thus optimised accordingly. When running with the biofuel blends, the exhaust composition changes, which may result in unfavourable consequences such as reducing catalyst efficiency due to different combustion products reducing catalyst activity [58,59]. Wiseman et al. [23] reported increased THC emissions relative to diesel when using these butyl blends. Whilst the C300h had a DOC installed, this would have been designed based on the use of EN 590 diesel; thus, the oxidation of increased THC emissions may not have been complete. The incomplete oxidation may have produced compounds such as propene, which is reported to occupy SCR catalytic sites, deactivating them and thus reducing conversion efficiency [58,59]. This would require further investigation to establish if the catalyst materials used in the C300h are more susceptible to deactivation with the exhaust gases generated from the butyl blends, along with investigating the composition of the exhaust gases pre- and post-DOC using the additional gas sampling probes installed into the exhaust (Figure 1) to establish how changes in gas composition influence SCR efficiency.

To investigate potential influences from the use of the electric motor as the sole means of propulsion, the total engine-off duration and number of ICE reignitions were analysed. No direct correlation could be found between the total mass of NO_X emitted and the number of reignitions or the engine-off duration. It would be expected that with the engine being off for long durations, there would be less total tailpipe NO_X. However, if the engine is off for long durations, the SCR would cool, reducing its removal efficiency. The influence of the individual engine-off periods on the SCR temperature and the subsequent NO_X emissions upon reignition requires further investigation. However, the lack of direct correlation between the total engine-off time and tailpipe NO_X emissions indicate that there are many other factors that contribute to changes in the NO_X emissions, including the SCR temperature, chemical deactivation due to changes in the engine-out emissions when running with the biofuel blends, and NO/NO_2 ratio. Therefore, SCR materials that are more suitable for use with oxygenated biofuels may require further development, along with further investigation of the role that the NO/NO_2 ratio post-DOC and other emissions in the exhaust have on the behaviour and efficiency of the SCR.

3.5. Influence of Biofuel Blends on Distance-Based PN Emission Factors for the Whole Trip

The PN emission factors from the C300h were below the Euro 6 limit of 6×10^{11} #/km for all fuel blends tested [25]. In an analogous manner to the CO emissions, the total PN emissions were reduced upon addition of the biofuel blends, as shown in Figure 18. For the two Bu10 blends, there were slight increases in the average PN emission factors during the rural and motorway phases relative to diesel. However, when accounting for the standard deviations, there are no discernible differences in the average total emission factors between the Bu10 blends and diesel, which could be due to equivalent DPF effectiveness for all the fuels. During the urban phase of the RDE, the PN emissions are skewed by the cold start PN emissions, as there are typically high tailpipe PN emissions that have not been

captured by the DPF. During the cold start period, the exhaust temperature pre-DPF is low (Figure 13). As a result, there is a low pressure drop between the DPF inlet and outlet, which reduces the particulate collection efficiency [60,61]. Once the exhaust is up to temperature, the pressure drop across the DPF increases and the particulate collection efficiency increases [60,61]. Therefore, any reductions in PN during the urban phase are likely to be due to lower engine-out emissions due to the addition of the biofuel blends.

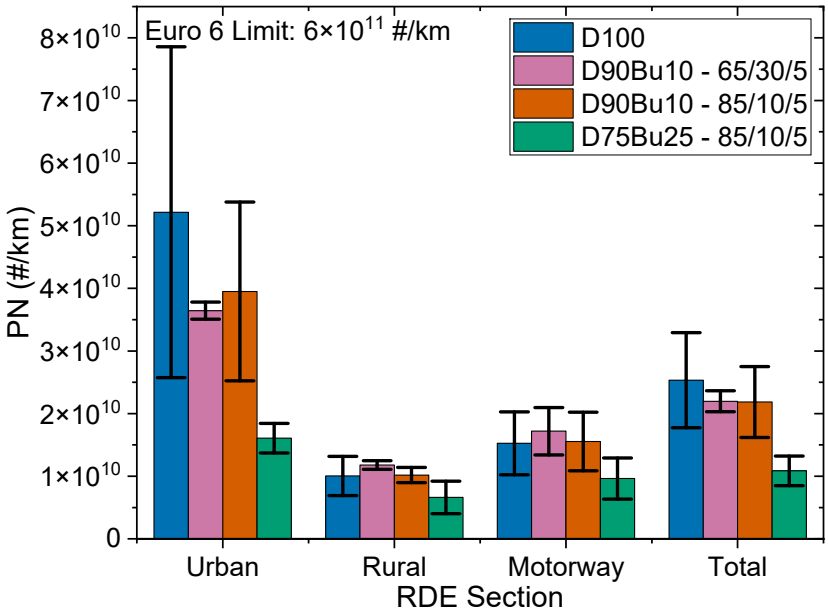

Figure 18. Comparison of PN emission factors from C300h for each RDE section with each fuel blend tested. Error bars are one standard deviation from the three repeats.

The average total PN emission factors were reduced by 13%, 14%, and 57% relative to diesel for D90Bu10 – 65/30/5, D90Bu10 – 85/10/5, and D75Bu25 – 85/10/5, respectively. The largest reductions were in the urban phase, with a 69% reduction for D75Bu25 – 85/10/5. The reductions in the urban phase and total emission factor for D75Bu25 – 85/10/5 were statistically significant at a 95% confidence limit when using the emissions from the three test runs. Reductions in PN emissions will be beneficial for air quality, particularly in an urban setting [13,62]. When the engine and exhaust have reached warm temperatures, such as in the rural and motorway sections, there is a less obvious trend in the PN emissions with the butyl blends. The two 10 vol% blends have comparable emissions factors to D100. However, D75Bu25 – 85/10/5 has a reduction in the emission factor for these two phases, which contributes to the reduction in the total emission factor for this fuel. However, any slight increases in PN may be due to the nature of the particles changing, as the number of particles may have increased, but the total mass of particles may have reduced as seen when these fuels were tested in gensets [21,23]. The results indicate that when the engine and exhaust after-treatment systems are warm, higher fractions of biofuel are needed to cause the reduction in the PN relative to diesel, as shown for the rural- and motorway-phase emission factors.

Figure 19 shows that the cumulative PN emissions during the RDE test are lower for the biofuel blends relative to diesel. It also shows a change in the nature of the cumulative PN profile when moving to the butyl blends. With D100, for two of the RDE trips, more than 50% of the total cumulative PN emissions occur during the cold start, as discussed in Section 3.2.3. On the other hand, for the biofuel blends, the cold start emissions accounted for 13–19%, 10–38%, and 6–30% of the total emissions for D90Bu10 – 65/30/5, D90Bu10 – 85/10/5, and D75Bu25 – 85/10/5, respectively. This reduction in PN emissions

further indicates the influence of the butyl blends on reducing the engine-out PN through a combination of increased fuel oxygen content, reduction in the formation of particulate precursors, and reduced net aromatic content of the fuel. This is also evident in Figure 18, where the urban section has the highest emission factor for all fuels (higher than the total PN emissions factor), and the largest reductions in PN relative to diesel are seen for the D75Bu25 – 85/10/5 blend. This is consistent with most of the tests using the butyl blends showing cold start contributions of less than 20% of the total PN emissions. For two of the trips with both D90Bu10 – 85/10/5 and D75Bu25 – 85/10/5, the increase in the cumulative PN is slower and more linear during the duration of the RDE, with only one trip for each of these fuels showing a more diesel-like sudden increase during the cold start period. For D75Bu25 – 85/10/5, the motorway phase caused the larger increase per second compared to the urban and rural phases (Figure 19d), as indicated by the increase in gradient for the cumulative PN curves at around 4500 s. The higher emissions in the motorway phase compared to the urban and rural phase is to be expected as higher quantities of fuel are being burnt whilst the engine is under a higher load, so there would inherently be more particles produced compared to lower load driving. Both Bu10 blends had slightly higher average motorway emission factors compared to D100 due to the higher spikes in emissions compared to diesel. However, we do not know the nature of the particles emitted from the vehicle as the OBS-ONE only counts total solid particles. If there was an increase in smaller particles, it may indicate that DPF efficiencies for removing smaller particles would need to improve, and this is likely to come with the new generation of DPFs for the upcoming Euro 7 emissions regulation [50].

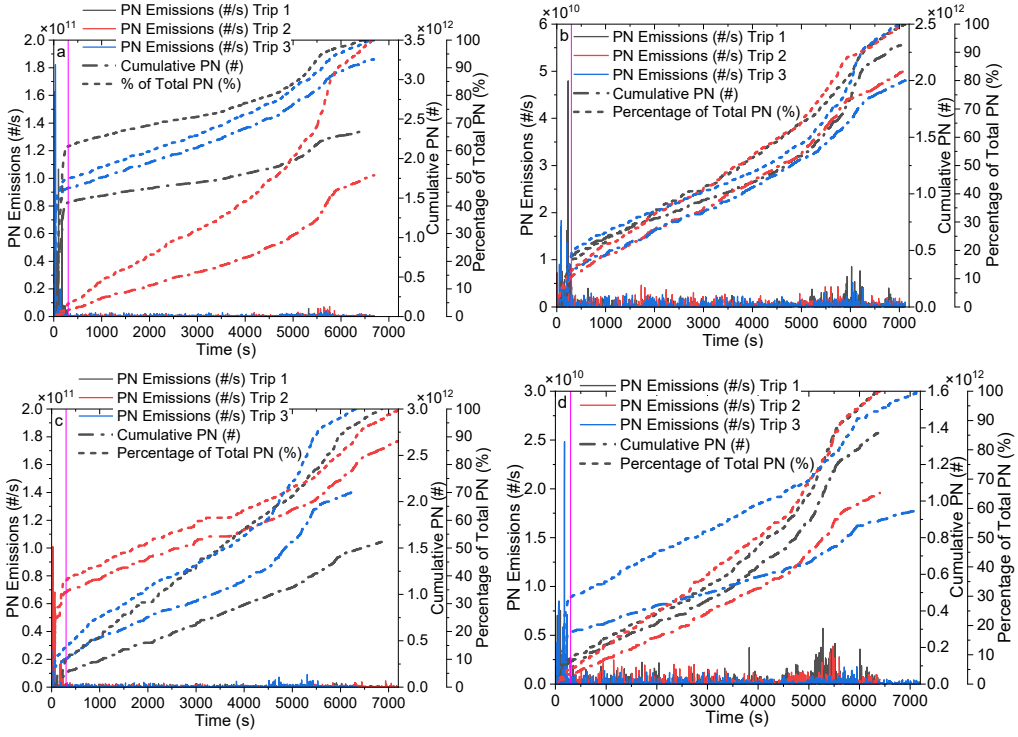

Figure 19. PN emissions, cumulative PN, and percentage of total PN emissions for three tests using the different fuels: (**a**) D100 trip 3, (**b**) D90Bu10 – 65/30/5 trip 1, (**c**) D90Bu10 – 85/10/5 trip 2, and (**d**) D75Bu25 – 85/10/5 trip 3. The pink vertical line is at 300 s, which is the end of the cold start period. Note the scales for PN emission on (**a**,**c**) are 1011 and (**b**,**d**) are 1010.

The efficiency of the DPF was further highlighted by a lack of a direct correlation between the total PN emitted and the number of ICE reignitions or the total PN emitted and the total engine-off duration. The lack of a direct correlation indicates that there

was no statistically significant influence of the utilisation of the electric motor and hybrid powertrain. Further investigation into the nature of the particles produced and pre- and post-DPF measurements are required to fully understand the influence of the utilisation of the electric motor on the particulate emissions when using diesel or the butyl blends.

The reductions in PN were expected, as when the three biofuel blends were tested in a genset engine, the total PN and $PM_{2.5}$ were reduced by up to 85% and 58%, respectively, for D75Bu25 – 85/10/5 compared to diesel when the engine was under load [23]. The emissions reductions in the RDE were not as high as those observed in the genset testing, but this could be due to the OBS-ONE measuring solid particles, and not total PN, as well as the lack of use of a DPF in the genset testing. However, studies by Wiseman et al. [23] and Antonetti et al. [21] demonstrated that total PN, $PM_{2.5}$, and fuel smoke number reduced when using these fuel blends in gensets. Therefore, the reductions from a vehicle under transient operation conditions were found to be consistent with previous tests.

Additionally, the reduction in PN is favourable for future applications, as the next generation of emissions standards are widening the size range of particles to be included in the PN measurement. Euro 7 will require the measurement of PN for particles >10 nm in diameter [50]. Therefore, the total measured PN will increase, and any overall reductions because of fuel changes may make meeting the limits in the future regulations more likely, even with redesigned after-treatment systems. It is also encouraging that the DPF was able to maintain high efficiencies for all fuel blends, leading to exhaust emissions well below limit values.

4. Conclusions

The results show the potential of advanced biofuel blends produced using alcoholysis processes to act as drop-in fuels within an existing diesel hybrid vehicle. The butyl blends tested could be used without any engine or fuel system modification, with minimal differences in vehicle drivability. The following conclusions can be drawn from this work.

- Ensuring that fuel blends were within the physical property limits for diesel, and were compatible with fuel system materials, ensured safe operation and reduced the likelihood of fuel system faults. This was evident by driving over 600 km on each fuel blend without any issues.
- Using the biofuel blends resulted in small fuel economy penalties of <5% relative to D100. Therefore, the use of the advanced biofuel blends should not cause a noticeable increase in refuelling frequency, alleviating potential concerns of end users.
- The use of the biofuel blends caused reductions in cold start PN and NO_X emissions relative to D100, making them attractive advanced biofuel blends to potentially displace diesel, since urban emissions of PN and NO_X have a significant impact on public health.
- Use of the biofuel blends led to reductions in trip total CO and PN emissions by up to 72% and 57%, respectively, when running with D75Bu25 – 85/10/5, which showed the largest reduction in all the blends relative to D100. The changes in CO and PN emissions, whilst using a DOC and DPF designed for the use of EN 590 diesel, highlights that the additional oxygen content, and the net reduction in the fuel aromatic content, was likely to have contributed to these reductions.
- The addition of the butyl blends to diesel caused some SCR deactivation, leading to an increase in total NO_X emission factors relative to D100 by up to 26% with D75Bu25 – 85/10/5. The average NOx removal fraction by the SCR reduced from 67% with D100 to 58% with D75Bu25 – 85/10/5, whereas the pre-SCR NO_X emissions were similar to or lower than those of D100 when running with the biofuel blends. Improved optimisation of SCR reagent injection strategies may therefore be required

when running with advanced biofuels. For the vehicle used in this work, the DOC and SCR catalyst brick sizes would have been selected based on the engine-out emissions when using EN 590 diesel fuels and, hence, may need redesigning for use with advanced biofuels. Investigation of material changes to the after-treatment system, potentially including the utilisation of more chemically and hydrothermally resilient materials, would also be useful.

- For the sample size of 12 used in this work, the total engine-off duration and the number of reignitions did not show statistically significant correlations with the total emissions of CO, NO_X, or PN. There was, however, a statistically significant correlation between the total NO_X emitted during the cold start period and the number of reignitions and the engine-off duration. These results indicate that the use of the electric motor over the whole trip may not have had a strong influence on the tailpipe emissions due to the presence of the exhaust after-treatment systems.
- Since the fuel blends tested here are shown to be compatible with an existing vehicle, and their properties can be tailored to meet selected existing fuel property limits, the utilisation of the butyl blends as drop-in fuels is a potential option that would help to decarbonise the existing diesel-based vehicle fleet, assuming that sustainable production methods were used. Because of current limitations on the types of permitted blending agents, without a new fuel standard, or changes to EN 590, it could be difficult to meet the mandated RED III advanced biofuel utilisation requirements [8,22].

Supplementary Materials: The following supporting information can be downloaded at: https://www.mdpi.com/article/10.3390/en19020308/s1. Table S1: ECU channels logged using Rebel LT and their logging frequencies. Table S2: Average fuel economy for each fuel tested. Table S3: Average total cumulative cold start pollutant emissions during the first 300 s of the test for each fuel blend. Table S4: Average CO emission factors for each RDE section for each fuel blend. Table S5: Average PN emission factors for each RDE section for each fuel blend. Table S6: Average NO_X emission factors for each RDE section for each fuel blend. Table S7. Average total mass of NO_X emitted measured with the pre- and post-SCR NO_X sensors and the OBS-ONE. Table S8. Average fraction of NO_X removed by SCR and the average total AdBlue Metering Mass.

Author Contributions: Conceptualization, A.S.T., H.L. and S.W.; methodology, A.S.T., H.L. and S.W.; software, K.R.; formal analysis, S.W.; investigation, S.W.; resources, A.S.T., H.L. and K.R.; data curation, S.W.; writing—original draft preparation, S.W.; writing—review and editing, A.S.T., H.L., K.R. and S.W.; visualisation, S.W. and K.R.; supervision, H.L. and A.S.T.; project administration, A.S.T. and H.L.; funding acquisition, A.S.T. and H.L. All authors have read and agreed to the published version of the manuscript.

Funding: This work was funded by UKRI EPSRC grant EP/T033088/1 and by UKRI STFC grant ST/Z51035X/1.

Data Availability Statement: The original contributions presented in this study are included in the article/Supplementary Materials. Further inquiries can be directed to the corresponding author(s).

Acknowledgments: The authors would like to thank the SusLABB project team for their support. Thanks to Scott Prichard, our research technician, for the support and manufacturing of parts. Thanks to Influx Technology Ltd., Bedford, UK, for their training and support when providing the Rebel LT logger. Thanks to Horiba MIRA, Nuneaton, UK, for conducting the WLTP. A special thanks to Horiba, Northampton, UK and Kevin Tully of Tully Engineering Ltd., Milton Keynes, UK, for providing us with the OBS-ONE and technical support and installation.

Conflicts of Interest: The authors declare no conflicts of interest.

Abbreviations

The following abbreviations are used in this manuscript:

Bu	Butyl Blend
CAZ	Clean Air Zone
CF	Conformity Factor
CN	Cetane Number
CO	Carbon Monoxide
CO_2	Carbon Dioxide
D	Diesel
DCN	Derived Cetane Number
DNBE	Di-*n*-butyl Ether
DOC	Diesel Oxidation Catalyst
DPF	Diesel Particulate Filter
ECU	Engine Control Unit
EGR	Exhaust Gas Recirculation
EU	European Union
FTIR	Fourier Transform Infrared
HC	Hydrocarbon
ICE	Internal Combustion Engine
LEZ	Low Emission Zone
MAW	Moving Average Window
*n*BL	*n*-Butyl Levulinate
*n*BuOH	*n*-Butanol
NO	Nitric Oxide
NO_2	Nitrogen Dioxide
NOVC	Not Off Vehicle Charging
NO_X	Nitrogen Oxides (NO + NO_2)
OVC	Off Vehicle Charging
PEMS	Portable Emissions Measurement System
$PM_{2.5}$	Particulate Matter with aerodynamic dynameters < 2.5 μm
PN	Particle Number
RDE	Real Driving Emissions
RED	Renewable Energy Directive
rpm	Revolutions per Minute
SCR	Selective Catalytic Reduction
UK	United Kingdom
ULEZ	Ultra-Low Emission Zone
WLTP	World Harmonised Light-Duty Test Procedure

References

1. International Energy Agency. Trucks and Buses. Available online: https://www.iea.org/ (accessed on 9 June 2025).
2. International Energy Agency. Transport. Available online: https://www.iea.org/ (accessed on 9 June 2025).
3. Suarez, J.; Tansini, A.; Ktistakis, M.A.; Marin, A.L.; Komnos, D.; Pavlovic, J.; Fontaras, G. Towards zero CO_2 emissions: Insights from EU vehicle on-board data. *Sci. Total Environ.* **2025**, *1001*, 180454. [CrossRef]
4. Zacharof, N.; Bitsanis, E.; Broekaert, S.; Fontaras, G. Reducing CO_2 Emissions of Hybrid Heavy-Duty Trucks and Buses: Paving the Transition to Low-Carbon Transport. *Energies* **2024**, *17*, 286. [CrossRef]
5. Tansini, A.; Marin, A.L.; Suarez, J.; Aguirre, N.F.; Fontaras, G. Learning from the real-world: Insights on light-vehicle efficiency and CO_2 emissions from long-term on-board fuel and energy consumption data collection. *Energy Convers. Manag.* **2025**, *335*, 119816. [CrossRef]
6. *(EU) 2023/851*; Regulation (EU) 2023/851 of the European Parliament and of the Council of 19 April 2023 Amending Regulation (EU) 2019/631 as Regards Strengthening the CO_2 Emission Performance Standards for New Passenger Cars and New Light Commercial Vehicles in Line with the Union's Increased Climate Ambition (Text with EEA Relevance). European Parliament: Strasbourg, France, 2023.

7. Department for Transport; Driver and Vehicle Licensing Agency. VEH1111: Licensed Vehicles at the End of the Year by Body Type and Year of First Use. 2025. Available online: https://www.gov.uk/ (accessed on 15 October 2025).
8. *(EU) 2023/2413*; Directive (EU) 2023/2413 of the European Parliament and of the Council of 18 October 2023 Amending Directive (EU) 2018/2001, Regulation (EU) 2018/1999 and Directive 98/70/EC as Regards the Promotion of Energy from Renewable Sources, and Repealing Council Directive (EU) 2015/652. European Parliament: Strasbourg, France, 2023. Available online: http://eur-lex.europa.eu/ (accessed on 23 April 2025).
9. Blasshofer, T.; Reichert, T. EU to Scrap Planned Ban on Combustion Engines, EPP's Weber Says. Available online: https://www.reuters.com/ (accessed on 14 December 2025).
10. *(EU) 2024/1610*; Regulation (EU) 2024/1610 of the European Parliament and of the Council of 14 May 2024 Amending Regulation (EU) 2019/1242 as Regards Strengthening the CO_2 Emission Performance Standards for New Heavy-Duty Vehicles and Integrating Reporting Obligations, Amending Regulation (EU) 2018/858 and Repealing Regulation (EU) 2018/956 (Text with EEA Relevance). European Parliament: Strasbourg, France, 2024.
11. Bergthorson, J.M.; Thomson, M.J. A Review of the Combustion and Emissions Properties of Advanced Transportation Biofuels and Their Impact on Existing and Future Engines. *Renew. Sustain. Energy Rev.* **2015**, *42*, 1393–1417. [CrossRef]
12. Huseynov, S.; Palma, M.A. Does California's Low Carbon Fuel Standards reduce carbon dioxide emissions? *PLoS ONE* **2018**, *13*, e0203167. [CrossRef]
13. Hooftman, N.; Messagie, M.; Van Mierlo, J.; Coosemans, T. A review of the European passenger car regulations—Real driving emissions vs local air quality. *Renew. Sustain. Energy Rev.* **2018**, *86*, 1–21. [CrossRef]
14. García-Contreras, R.; Soriano, J.A.; Fernández-Yáñez, P.; Sánchez-Rodríguez, L.; Mata, C.; Gómez, A.; Armas, O.; Cárdenas, M.D. Impact of regulated pollutant emissions of Euro 6d-Temp light-duty diesel vehicles under real driving conditions. *J. Clean. Prod.* **2021**, *286*, 124927. [CrossRef]
15. Park, Y.-K.; Kim, B.-S. Catalytic removal of nitrogen oxides (NO, NO_2, N_2O) from ammonia-fueled combustion exhaust: A review of applicable technologies. *Chem. Eng. J.* **2023**, *461*, 141958. [CrossRef]
16. Wiseman, S.; Michelbach, C.A.; Li, H.; Tomlin, A.S. Predicting the physical properties of three-component lignocellulose derived advanced biofuel blends using a design of experiments approach. *Sustain. Energy Fuels* **2023**, *7*, 5283–5300. [CrossRef]
17. Alamgir Ahmad, K.; Haider Siddiqui, M.; Pant, K.K.; Nigam, K.D.P.; Shetti, N.P.; Aminabhavi, T.M.; Ahmad, E. A critical review on suitability and catalytic production of butyl levulinate as a blending molecule for green diesel. *Chem. Eng. J.* **2022**, *447*, 137550. [CrossRef]
18. Raspolli Galletti, A.M.; Lorè, R.; Licursi, D.; Di Fidio, N.; Antonetti, C.; Fulignati, S. Insights on butyl levulinate bio-blendstock: From model sugars to paper mill waste cellulose as feedstocks for a sustainable catalytic butanolysis process. *Catal. Today* **2023**, *418*, 114054. [CrossRef]
19. Nahil, M.A.; Aboelazayem, O.; Wiseman, S.; Herar, N.; Dupont, V.; Alazzawi, A.; Tomlin, A.S.; Ross, A.B. Production and Optimisation of Oxygenated Biofuel Blend Components via the Ethanolysis of Lignocellulosic Biomass: A Response Surface Methodology. *Energies* **2025**, *18*, 2985. [CrossRef]
20. O'Shea, A.; McNamara, C.; Rao, P.; Howard, M.; Ghanni, M.R.; Dooley, S. A hierarchical surrogate approach to biomass ethanolysis reaction kinetic modelling. *React. Chem. Eng.* **2025**, *10*, 344–359. [CrossRef]
21. Antonetti, C.; Gori, S.; Licursi, D.; Pasini, G.; Frigo, S.; Lopez, M.; Parajo, J.C.; Galletti, A.M.R. One-Pot Alcoholysis of the Lignocellulosic Eucalyptus nitens Biomass to n-Butyl Levulinate, a Valuable Additive for Diesel Motor Fuel. *Catalysts* **2020**, *10*, 509. [CrossRef]
22. *BS EN 590:2022*; Automotive Fuels—Diesel—Requirements and Test Methods. BSI: Milton Keynes, UK, 2022. Available online: https://bsol.bsigroup.com/ (accessed on 12 October 2022).
23. Wiseman, S.; Li, H.; Tomlin, A.S. Combustion and Emission Performance from the use of Acid-catalysed Butanol Alcoholysis Derived Advanced Biofuel Blends in a Compression Ignition Engine. In Proceedings of the WCX SAE World Congress Experience, Detroit, MI, USA, 8–10 April 2025; SAE Technical Paper 2025-01-8445, 2025. [CrossRef]
24. Reif, K.; Dietsche, K.-H. *Automotive Handbook*, 9th ed.; Reif, K., Dietsche, K.-H., Eds.; Robert Bosch GmbH: Karlsruhe, Germany, 2014.
25. *(EU) No 459/2012*; Commission Regulation (EU) No 459/2012 of 29 May 2012 Amending Regulation (EC) No 715/2007 of the European Parliament and of the Council and Commission Regulation (EC) No 692/2008 as Regards Emissions from Light Passenger and Commercial Vehicles (Euro 6) Text with EEA Relevance; 32012R0459. European Commission: Brussels, Belgium, 2012.
26. *(EC) No 715/2007*; Regulation (EC) No 715/2007 of the European Parliament and of the Council of 20 June 2007 on Type Approval of Motor Vehicles with Respect to Emissions from Light Passenger and Commercial Vehicles (Euro 5 and Euro 6) and on Access to Vehicle Repair and Maintenance Information. European Parliament: Strasbourg, France, 2007.
27. DieselNet. EU: Cars and Light Trucks. Available online: https://dieselnet.com (accessed on 24 October 2025).
28. Reşitoğlu, İ.A.; Altinişik, K.; Keskin, A. The pollutant emissions from diesel-engine vehicles and exhaust aftertreatment systems. *Clean Technol. Environ. Policy* **2015**, *17*, 15–27. [CrossRef]

29. Franco, V.; Zacharopoulou, T.; Hammer, J.; Schmidt, H.; Mock, P.; Weiss, M.; Samaras, Z. Evaluation of Exhaust Emissions from Three Diesel-Hybrid Cars and Simulation of After-Treatment Systems for Ultralow Real-World NOx Emissions. *Environ. Sci. Technol.* **2016**, *50*, 13151–13159. [CrossRef]
30. Tipanluisa, L.; Prati, M.V.; Costagliola, M.A. Impact of diesel/renewable fuels blend on gaseous and particle emissions of a light-duty vehicle under real driving emissions. *Renew. Energy* **2024**, *230*, 120819. [CrossRef]
31. Wiseman, S.; Ropkins, K.; Li, H.; Tomlin, A.S. Influence of Blending *n*-Butanol Alcoholysis Derived Advanced Biofuels with Diesel on the Regulated Emissions from a Diesel Hybrid Vehicle. In Proceedings of the European Combustion Meeting 2025, Edinburgh, Scotland, 7–10 April 2025.
32. Horiba. OBS-ONE GS Unit. Available online: https://www.horiba.com (accessed on 5 February 2024).
33. Horiba. OBS-ONE PN Unit. Available online: https://www.horiba.com (accessed on 5 February 2024).
34. McNamara, C.; O'Shea, A.; Rao, P.; Ure, A.; Ayarde-Henríquez, L.; Ghaani, M.R.; Ross, A.; Dooley, S. Steady states and kinetic modelling of the acid-catalysed ethanolysis of glucose, cellulose, and corn cob to ethyl levulinate. *Energy Adv.* **2024**, *3*, 1439–1458. [CrossRef] [PubMed]
35. Flannelly, T.; Dooley, S.; Leahy, J.J. Reaction Pathway Analysis of Ethyl Levulinate and 5-Ethoxymethylfurfural from d-Fructose Acid Hydrolysis in Ethanol. *Energy Fuels* **2015**, *29*, 7554–7565. [CrossRef]
36. *BS 2869:2017 + A1:2022*; Fuel Oils for Agricultural, Domestic and Industrial Engines and Boilers. BSI: Milton Keynes, UK, 2022. Available online: https://bsol.bsigroup.com/ (accessed on 12 October 2022).
37. *EN ISO 3838:2004 + A1:2023*; Crude Petroleum and Liquid or Solid Petroleum Products—Determination of Density or Relative Density—Capillary-Stoppered Pyknometer and Graduated Bicapillary Pyknometer Methods. BSI: Milton Keynes, UK, 2024. Available online: https://bsol.bsigroup.com/ (accessed on 5 March 2024).
38. Yanowitz, J.; Ratcliff, M.A.; McCormick, R.L.; Taylor, J.D.; Murphy, M.J. *Compendium of Experimental Cetane Numbers*; National Renewable Energy Laboratory (NREL): Golden, CO, USA, 2017.
39. Linstrom, P.J.; Mallard, W.G. (Eds.) *NIST Chemistry WebBook, NIST Standard Reference Database Number 69*; 20899; National Institute of Standards and Technology: Gaithersburg, MD, USA, 2025.
40. Nikitin, E.D.; Popov, A.P.; Bogatishcheva, N.S.; Faizullin, M.Z. Critical temperatures and pressures, heat capacities, and thermal diffusivities of levulinic acid and four n-alkyl levulinates. *J. Chem. Thermodyn.* **2019**, *135*, 233–240. [CrossRef]
41. Christensen, E.; Williams, A.; Paul, S.; Burton, S.; McCormick, R.L. Properties and Performance of Levulinate Esters as Diesel Blend Components. *Energy Fuels* **2011**, *25*, 5422–5428. [CrossRef]
42. Çelebi, Y.; Aydın, H. An overview on the light alcohol fuels in diesel engines. *Fuel* **2019**, *236*, 890–911. [CrossRef]
43. Wang, J.; Sun, L.; Luan, P.; Wu, Y.; Cheng, Z.; Zhang, Z.; Kong, X.; Liu, H.; Chen, G. Effect of diesel blended with di-n-butyl ether/1-octanol on combustion and emission in a heavy-duty diesel engine. *Environ. Pollut.* **2022**, *311*, 119976. [CrossRef]
44. National Renewable Energy Laboratory. *Co-Optimization of Fuels & Engines: Fuel Properties Database*; National Renewable Energy Laboratory: Golden, CO, USA, 2016.
45. *(EU) 2018/1832*; Commission Regulation (EU) 2018/1832 of 5 November 2018 Amending Directive 2007/46/EC of the European Parliament and of the Council, Commission Regulation (EC) No 692/2008 and Commission Regulation (EU) 2017/1151 for the Purpose of Improving the Emission Type Approval Tests and Procedures for Light Passenger and Commercial Vehicles, Including Those for in-Service Conformity and Real-Driving Emissions and Introducing Devices for Monitoring the Consumption of Fuel and Electric Energy (Text with EEA Relevance) Text with EEA Relevance. European Commission: Brussels, Belgium, 2018.
46. Ropkins, K. *pems.utils: Data Handling, Analysis and Visualisation Tools for Data from Portable Emissions Monitoring Systems and Other Mobile Sources*, R package version 0.3.0.8. 2025. [CrossRef]
47. R Core Team. *R: A Language and Environment for Statistical Computing*, 4.4; R Foundation for Statistical Computing: Vienna, Austria, 2024. Available online: https://www.R-project.org (accessed on 30 November 2024).
48. Akita, M. Real-time Fuel Consumption Measurement Using Raw Exhaust Flow Meter and Zirconia AFR Sensor. *Readout Horiba Tech. Rep.* **2014**, *42*, 70–75. [CrossRef]
49. Thomas, D.; Li, H.; Ropkins, K.; Wang, X.; Ge, Y. Investigating the engine behavior of a hybrid vehicle and its impact on regulated emissions during on-road testing. In Proceedings of the JSAE/SAE 2019 Powertrains, Fuels and Lubricants, Kyoto, Japan, 26–29 August 2019; SAE Technical Paper 2019-01-2199, 2019. [CrossRef]
50. *(EU) 2024/1257*; Regulation (EU) 2024/1257 of the European Parliament and of the Council of 24 April 2024 on Type-Approval of Motor Vehicles and Engines and of Systems, Components and Separate Technical Units Intended for Such Vehicles, with Respect to Their Emissions and Battery Durability (Euro 7), Amending Regulation (EU) 2018/858 of the European Parliament and of the Council and Repealing Regulations (EC) No 715/2007 and (EC) No 595/2009 of the European Parliament and of the Council, Commission Regulation (EU) 582/2011, Commission Regulation (EU) 2017/1151, Commission Regulation (EU) 2017/2400 and Commission Implementing Regulation (EU) 2022/1362. European Parliament: Strasbourg, France, 2024.

51. Wang, X.-R.; Li, H.-M.; Li, G.-X.; Gao, Y.; Huo, H.-B.; Zhang, X.-Q.; Wang, Z.-G.; Bai, H.-L. Experimental investigation of atomization characteristics at low temperature environments during diesel engine cold start. *J. Energy Inst.* **2024**, *113*, 101544. [CrossRef]
52. Zeldovich, J. The Oxidation of Nitrogen in Combustion and Explosions. *Acta Physiochem* **1946**, *21*, 577–628.
53. Frigo, S.; Pasini, G.; Caposciutti, G.; Antonelli, M.; Galletti, A.M.R.; Gori, S.; Costi, R.; Arnone, L. Utilisation of advanced biofuel in CI internal combustion engine. *Fuel* **2021**, *297*, 120742. [CrossRef]
54. Chen, H.; Kwong, J.C.; Copes, R.; Tu, K.; Villeneuve, P.J.; van Donkelaar, A.; Hystad, P.; Martin, R.V.; Murray, B.J.; Jessiman, B.; et al. Living near major roads and the incidence of dementia, Parkinson's disease, and multiple sclerosis: A population-based cohort study. *Lancet* **2017**, *389*, 718–726. [CrossRef]
55. Gmbh, R.B. (Ed.) *Diesel-Engine Management*, 4th ed.; Completely Revised and Extended; Robert Bosch Gmbh: Plochingen, Germany, 2005.
56. Thomas, D.B. Real World Driving Emissions from Hybrid Electric Vehicles and the Impact of Biofuels. Ph.D. Thesis, University of Leeds, Leeds, UK, 2020.
57. Kitamura, T.; Ito, T.; Senda, J.; Fujimoto, H. Mechanism of smokeless diesel combustion with oxygenated fuels based on the dependence of the equivalence ration and temperature on soot particle formation. *Int. J. Engine Res.* **2002**, *3*, 223–248. [CrossRef]
58. Zhang, S.; Pang, L.; Chen, Z.; Ming, S.; Dong, Y.; Liu, Q.; Liu, P.; Cai, W.; Li, T. Cu/SSZ-13 and Cu/SAPO-34 catalysts for deNOx in diesel exhaust: Current status, challenges, and future perspectives. *Appl. Catal. A Gen.* **2020**, *607*, 117855. [CrossRef]
59. Jin, M.; Wang, P.; Li, Z.; Li, K.; Liu, Y. Deactivation mechanism of Cu-based zeolites (AEI, SSZ-13, ZSM-5, BEA) for NH3-SCR by hydrocarbons deposition species. *Fuel* **2024**, *365*, 131215. [CrossRef]
60. Kobashi, Y.; Oooka, S.; Jiang, L.; Goto, J.; Ogawa, H.; Shibata, G. An Investigation of the Transient DPF Pressure Drop under Cold Start Conditions in Diesel Engines. In Proceedings of the International Powertrains, Fuels & Lubricants Meeting, Beijing, China, 16–19 October 2017. SAE Technical Paper 2017-01-2372, 2017. [CrossRef]
61. Wirojsakunchai, E.; Schroeder, E.; Kolodziej, C.; Foster, D.E.; Schmidt, N.; Root, T.; Kawai, T.; Suga, T.; Nevius, T.; Kusaka, T. Detailed Diesel Exhaust Particulate Characterization and Real-Time DPF Filtration Efficiency Measurements During PM Filling Process. In Proceedings of the SAE World Congress & Exhibition, Detroit, MI, USA, 16–19 April 2007; SAE Technical Paper 2007-01-0320, 2007. [CrossRef]
62. Kampa, M.; Castanas, E. Human health effects of air pollution. *Environ. Pollut.* **2008**, *151*, 362–367. [CrossRef]